HHS Public Access

Author manuscript

Cell Rep. Author manuscript; available in PMC 2021 April 07.

Published in final edited form as:

Cell Rep. 2021 March 23; 34(12): 108899. doi:10.1016/j.celrep.2021.108899.

Activity- and sleep-dependent regulation of tonic inhibition by Shisa7

Kunwei Wu[1], **Wenyan Han**[1], **Qingjun Tian**[1], **Yan Li**[2], **Wei Lu**[1,3,*]

[1]Synapse and Neural Circuit Research Section, National Institute of Neurological Disorders and Stroke, National Institutes of Health, Bethesda, MD 20892, USA

[2]Proteomics Core Facility, National Institute of Neurological Disorders and Stroke, National Institutes of Health, Bethesda, MD 20892, USA

[3]Lead contact

SUMMARY

Tonic inhibition mediated by extrasynaptic γ-aminobutyric acid type A receptors ($GABA_ARs$) critically regulates neuronal excitability and brain function. However, the mechanisms regulating tonic inhibition remain poorly understood. Here, we report that Shisa7 is critical for tonic inhibition regulation in hippocampal neurons. In juvenile Shisa7 knockout (KO) mice, α5-$GABA_AR$-mediated tonic currents are significantly reduced. Mechanistically, Shisa7 is crucial for α5-$GABA_AR$ exocytosis. Additionally, Shisa7 regulation of tonic inhibition requires protein kinase A (PKA) that phosphorylates Shisa7 serine 405 (S405). Importantly, tonic inhibition undergoes activity-dependent regulation, and Shisa7 is required for homeostatic potentiation of tonic inhibition. Interestingly, in young adult Shisa7 KOs, basal tonic inhibition in hippocampal neurons is unaltered, largely due to the diminished α5-$GABA_AR$ component of tonic inhibition. However, at this stage, tonic inhibition oscillates during the daily sleep/wake cycle, a process requiring Shisa7. Together, these data demonstrate that intricate signaling mechanisms regulate tonic inhibition at different developmental stages and reveal a molecular link between sleep and tonic inhibition.

Graphical abstract

*Correspondence: luw4@mail.nih.gov.

AUTHOR CONTRIBUTIONS

K.W. and W.L. designed the project, and W.L. supervised the project. K.W. performed imaging, biochemical, electrophysiological, and behavioral experiments. K.W. and Y.L. performed MS assays. W.H. performed some of electrophysiological assays in HEK293T cells. Q.T performed neuronal cultures and *in utero* electroporation (IUE). W.L. and K.W. wrote the manuscript, and all authors read and commented on the manuscript.

DECLARATION OF INTERESTS

The authors declare no competing interests.

SUPPLEMENTAL INFORMATION

Supplemental information can be found online at https://doi.org/10.1016/j.celrep.2021.108899.

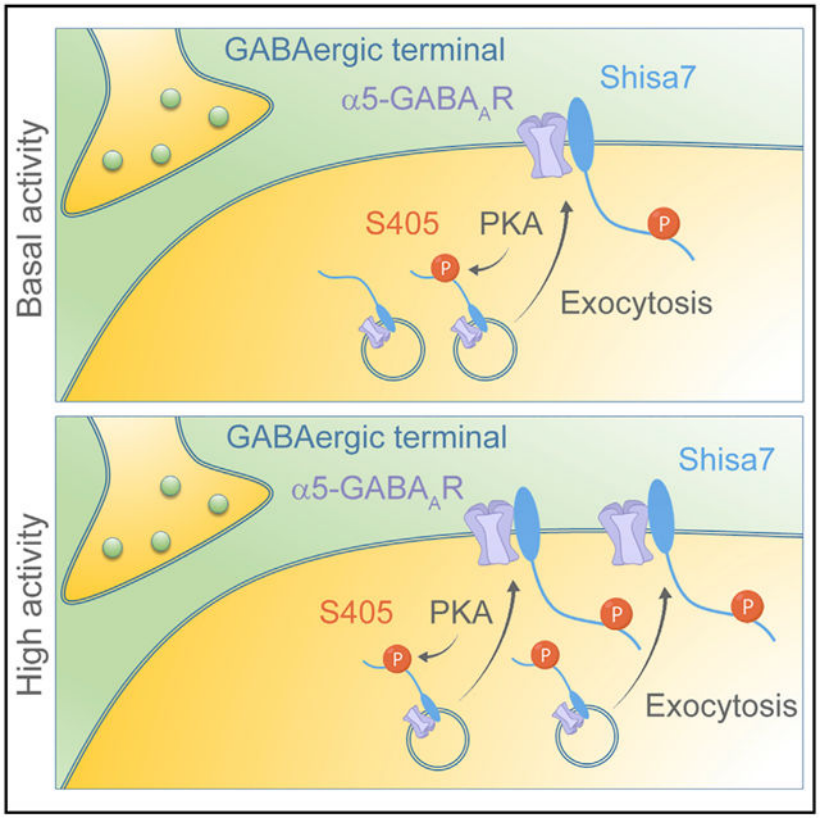

In brief

Wu et al. discover a critical role of Shisa7 in the regulation of tonic inhibition in hippocampal neurons and find that PKA phosphorylates Shisa7 to modulate activity-dependent regulation of tonic inhibition. They also show that Shisa7 is involved in tonic inhibition regulation over the daily sleep/wake cycle.

INTRODUCTION

γ-Aminobutyric acid (GABA), the major inhibitory neurotransmitter in the brain, acts primarily on GABA type A receptors (GABA$_A$Rs) to mediate fast inhibitory synaptic transmission. GABA$_A$Rs are ligand-gated pentameric anion channels assembled from various combinations of 19 subunits, α(1–6), β(1–3), γ(1–3), δ, ε, θ, π, and ρ(1–3), although most GABA$_A$Rs in the brain consist of two α subunits, two β subunits, and one γ subunit (Olsen and Sieghart, 2008). Due to their ubiquitous distribution and importance in the regulation of neuronal excitability and neural circuit information processing, GABA$_A$Rs play critical roles in virtually all brain functions (Jacob et al., 2008; Luscher et al., 2011; Vithlani et al., 2011). In addition, dysregulations of GABA$_A$R-mediated processes have been implicated in a number of devastating brain disorders, such as epilepsy, autism, and Alzheimer's disease (Braat and Kooy, 2015; Hines et al., 2012; Jacob et al., 2008). Thus, it is crucial to understand the molecular mechanisms underlying the regulation of GABA$_A$R-mediated inhibition.

The vast majority of fast inhibitory transmission in the brain is mediated by $GABA_A$Rs containing α1–3. In contrast, $GABA_A$Rs containing α4–6 are largely localized at the perisynaptic and extrasynaptic membranes in neurons (Belelli et al., 2009; Farrant and Nusser, 2005). These receptors are slowly desensitizing channels with high affinity to GABA and can be tonically and persistently activated by the low levels of ambient GABA in the brain. This tonic form of inhibition has been shown to critically modulate neuronal excitability, neural circuit function, and behavior (Belelli et al., 2009; Brickley and Mody, 2012; Farrant and Nusser, 2005; Lee and Maguire, 2014). However, while the molecular and cellular mechanisms underlying the regulation of synaptic $GABA_A$Rs have been extensively investigated (Jacob et al., 2008; Luscher et al., 2011; Vithlani et al., 2011), the regulatory mechanisms for tonic inhibition are less understood, warranting more investigation.

In hippocampal CA1 pyramidal neurons, the majority of tonic inhibition is mediated by α5-containing $GABA_A$Rs (α5-$GABA_A$Rs) (Caraiscos et al., 2004; Glykys et al., 2008), while the remaining amount of tonic inhibition is mediated by δ-containing $GABA_A$Rs (δ-$GABA_A$Rs) that are in complex with the α4 subunit (Glykys et al., 2008). A substantial number of α5-$GABA_A$Rs in hippocampal pyramidal neurons are localized at the extrasynaptic membranes and form discrete clusters through the interaction with radixin (Hausrat et al., 2015; Loebrich et al., 2006). In addition, acute increases in activity promote the activation of L-type calcium channels, which triggers further intracellular signaling cascades that result in phosphorylation of β3 by Ca^{2+}/calmodulin-dependent protein kinase II (CaMKII) and subsequently enhance membrane insertion of α5β3-$GABA_A$Rs (Saliba et al., 2012). Accumulating evidence from both genetic and pharmacological studies has also demonstrated that α5-$GABA_A$R-mediated tonic inhibition is critical for excitatory synaptic plasticity, neuronal network activity, and learning and memory and implicated in a number of brain disorders (Brickley and Mody, 2012; Glykys and Mody, 2007; Jacob, 2019; Martin et al., 2009; Mohamad and Has, 2019). Indeed, rare missense mutations in the α5 subunit have been identified in numerous patients with neurological and psychiatric disorders (Butler et al., 2018; Hernandez et al., 2019; Hodges et al., 2014). Furthermore, preclinical studies demonstrate that allosteric modulators that target α5-$GABA_A$Rs could be potentially therapeutic candidates for use in neurodevelopmental and neuropsychiatric disorders (Jacob, 2019; Mohamad and Has, 2019). However, despite the importance of α5-$GABA_A$R-mediated tonic inhibition in neuronal physiology and animal behaviors, the molecular mechanisms underlying trafficking and activity-dependent regulation of α5-$GABA_A$Rs and tonic inhibition currently remain poorly understood.

We recently identified a $GABA_A$R auxiliary subunit, Shisa7, which is a single-pass transmembrane protein that interacts with either α1- or α2-$GABA_A$Rs and thereby regulates inhibitory synaptic transmission (Han et al., 2019). Here, we report that Shisa7 also plays a critical role in the regulation of tonic inhibition in hippocampal CA1 neurons. In the juvenile Shisa7 knockout (KO) mice, both α5-$GABA_A$R exocytosis and tonic inhibition are significantly reduced. Furthermore, Shisa7-dependent regulation of tonic inhibition requires protein kinase A (PKA) that phosphorylates Shisa7 at serine 405 (S405). Importantly, tonic inhibition undergoes Shisa7-dependent homeostatic upregulation, revealing a previously uncharacterized form of neuronal plasticity. At the behavioral level in young adult mice, the daily sleep/wake oscillation regulates tonic inhibition in a Shisa7-dependent manner, a

process requiring the modulation at Shisa7 S405. Together, these data characterize critical molecular pathways regulating tonic inhibition and demonstrate how behavioral processes engage neuronal molecular signaling to modulate neural inhibition in the brain.

RESULTS

Tonic inhibitory currents are reduced in Shisa7 KO hippocampal neurons

To measure tonic inhibition, we performed whole-cell voltage-clamp recordings in hippocampal cultures. Application of bicuculline (BIC; 20 μM), a competitive antagonist of $GABA_A$Rs, to cultured neurons readily reduced baseline holding currents, revealing tonic currents mediated by extrasynaptic $GABA_A$Rs (Figure 1A). To account for the effect of cell size on tonic currents, we normalized tonic currents by the cell membrane capacitance, which did not significantly differ between wild-type (WT) and Shisa7 KO neurons (Figure S1). We found that compared to WT neurons, tonic currents in Shisa7 KO hippocampal neurons were significantly reduced (Figures 1A and S1A). In addition to cultured neurons, we measured tonic currents in acute hippocampal slices prepared from postnatal day 16 (P16) to P21 juvenile WT or Shisa7 KO mice. We found that $GABA_A$R-mediated tonic currents were substantially reduced in hippocampal CA1 neurons from Shisa7 KO mice (Figures 1B and S1B). Similarly, tonic currents were smaller in dentate gyrus (DG) granule cells in Shisa7 KO mice as compared to WT mice (Figures 1C and S1C), showing the importance of Shisa7 in the regulation of tonic inhibition in different hippocampal cell types. Together, these data demonstrate a critical role of Shisa7 in the regulation of tonic inhibition in hippocampal neurons.

Previous work has shown that extrasynaptic α5-$GABA_A$Rs mediate the majority of tonic inhibition in hippocampal CA1 neurons (Caraiscos et al., 2004; Glykys et al., 2008). Thus, we explored the role of Shisa7 regulation in both α5-$GABA_A$Rs-dependent and independent components of tonic currents in these neurons. Similar to previous reports (Caraiscos et al., 2004; Glykys et al., 2008), application of L-655,708, a potent α5-$GABA_A$R inverse agonist (Quirk et al., 1996), strongly reduced tonic inhibitory currents by ~70% in WT CA1 neurons (Figure 1D). Interestingly, in Shisa7 KO CA1 neurons, L-655,708-sensitive components of tonic currents were significantly reduced, while there was little change in L-655,708-insensitive tonic currents (Figure 1D). In hippocampal CA1 neurons, L-655,708-insensitive tonic inhibitory currents are largely mediated by δ-$GABA_A$Rs (Glykys et al., 2008). THIP (4,5,6,7-tetrahydroxyisoxazole [4,5-c]pyridine-3-ol), a $GABA_A$R agonist with a preference for δ-$GABA_A$Rs (Brown et al., 2002), evoked a similar amount of currents in WT and Shisa7 KO CA1 neurons (Figure 1E), showing that Shisa7 KO did not alter δ-$GABA_A$R-mediated currents. Collectively, these data indicate that Shisa7 KO reduces tonic inhibition mediated by α5-$GABA_A$R, but not δ-$GABA_A$Rs, in hippocampal CA1 neurons.

Shisa7 interacts with α5-$GABA_A$Rs and regulates receptor trafficking

We have recently shown that Shisa7 can be co-immunoprecipitated with α1- and α2-$GABA_A$Rs and promotes trafficking of these receptors to the cell surface and inhibitory synapses (Han et al., 2019). We thus examined whether Shisa7 could also interact with α5-$GABA_A$Rs. In HEK293T cells, we found that GFP-tagged α5 (α5-GFP) was co-

immunoprecipitated with Flag-tagged Shisa7 (Flag-Shisa7) from cells co-transfected with both constructs, but not from those transfected with either plasmid alone (Figures 2A and S2A). Similarly, in detergent-solubilized mouse hippocampal lysates, the α5 subunit was detected in the Shisa7 immunoprecipitates (Figures 2B and S2B). Interestingly, neither α4 nor δ subunits were co-immunoprecipitated with Shisa7 (Figure 2B), showing that Shisa7 is associated with α5-, but not α4- or δ-, $GABA_A$Rs in the hippocampus.

We then examined whether Shisa7 regulated α5-$GABA_A$R trafficking. In HEK293T cells, co-expression of Shisa7 with α5β3γ2 receptors significantly increased surface levels, total levels, and surface to total ratio of α5 expression (Figure 2C). Similarly, GABA-evoked α5β3γ2-mediated whole-cell currents were significantly increased in HEK293T cells co-expressing Shisa7 compared to cells co-expressing GFP (Figure 2D). Thus, Shisa7 promotes α5-$GABA_A$R trafficking to the cell surface in heterologous cells. In hippocampal cultures, we found that surface levels of α5 were significantly reduced in Shisa7 KO neurons compared to WT neurons (Figure 2E). In addition, total α5 expression was reduced in Shisa7 KO neurons (Figure 2E), suggesting that Shisa7 may play a role in the regulation of α5 expression and/or stability in hippocampal neurons. Furthermore, the surface to total ratio of α5 expression was significantly decreased in Shisa7 KO neurons (Figure 2E), indicating that α5-$GABA_A$Rs trafficking to the neuronal surface is impaired in neurons lacking Shisa7. Collectively, these data demonstrate that Shisa7 is important for α5-$GABA_A$R trafficking to the cell surface.

The reduction of the surface levels of α5 in Shisa7 KO neurons might involve increased endocytosis of surface α5 or reduced exocytosis of intracellular α5. To differentiate between these possible scenarios, we first performed antibody-feeding experiments to label surface and internalized endogenous α5 in live hippocampal cultures and examined α5 endocytosis in WT and Shisa7 KO neurons. We found that Shisa7 KO did not significantly change α5 internalization (Figure S2D). We then combined fluorescence recovery after photobleaching (FRAP) with fluorescence loss in photobleaching (FLIP) to investigate exocytosis of superecliptic pHluorin-tagged α5 (SEP-α5) to measure the receptor exocytosis. In this experiment, repetitive photobleaching occurred at dendritic regions bilateral to the central FRAP area, thus excluding laterally diffusing SEP-α5 to the central area and allowing the measurement of newly exocytosed SEP-α5 (Figures 2F and S2E). We found that while SEP-α5 expressed in WT neurons showed a substantial recovery within 5 min after photobleaching, much smaller fluorescence recovery of SEP-α5 was observed in Shisa7 KO neurons (Figures 2F and 2G), indicating that Shisa7 KO reduces α5 exocytosis.

Protein kinases regulate tonic inhibition

What are the molecular mechanisms underlying the regulation of tonic inhibition by Shisa7? Protein phosphorylation has been shown to play critical roles in regulating dynamic trafficking of neurotransmitter receptors (Connelly et al., 2013; Lu and Roche, 2012; Nakamura et al., 2015). To explore the potential role of protein kinases in the regulation of tonic inhibition, we performed pharmacological inhibition assays in hippocampal cultures and measured tonic inhibitory currents. We found that pharmacological inhibition of PKA, protein kinase C (PKC), or CaMKII led to a significant reduction of tonic currents in WT

neurons (Figure 3A), showing that tonic inhibition is sensitive to activities of a variety of protein kinases. Strikingly, in Shisa7 KO neurons, although blockade of CaMKII activity still decreased tonic inhibitory currents, the effects of inhibition of PKA or PKC activities on tonic currents were abolished (Figure 3A), indicating that those kinases modulate tonic inhibition through Shisa7.

PKA phosphorylates Shisa7 to regulate α5 exocytosis and tonic inhibition

Given that either PKA or PKC requires Shisa7 to regulate tonic inhibition, we hypothesized that Shisa7 was a phosphorylation substrate of PKA or PKC. To this end, we purified glutathione S-transferase (GST) fusion to Shisa7 C-terminal (C-tail) fragments and performed an *in vitro* phosphorylation assay with recombinant PKA or PKC. We then utilized liquid chromatograph coupled to tandem mass spectrometry (LC-MS/MS) to identify phosphorylated residues. We found several serine or threonine residues on the C-tail of Shisa7 that were substrates of PKA and/or PKC *in vitro* (Figure 3B). To further evaluate whether these phosphorylation events occurred *in vivo*, we performed an immunoprecipitation assay to pulldown endogenous Shisa7 from mouse hippocampal lysates and used LC-MS/MS to detect phosphorylated residues of neuronal Shisa7. We identified two phosphorylated serine residues (S405 and S430) in neuronal Shisa7 that were substrates of PKA (Figures 3B and 3C), showing that these two residues can be phosphorylated both *in vitro* and *in vivo*.

In addition to the two above-mentioned serine residues that we identified *in vivo*, recent studies identified that Shisa7 S306 was phosphorylated in mouse brain lysates (Li et al., 2016; Wang et al., 2018). We thus sought to determine the role of phosphorylation at these three residues (i.e., S306, S405, and S430) in tonic inhibition. In hippocampal cultures prepared from Shisa7 KO mice, expression of WT Shisa7 significantly increased tonic inhibitory currents (Figures 4A–4C). In contrast, expression of the Shisa7 mutant lacking the majority of C-tail (Shisa7 ΔC) did not rescue the tonic current deficit (Figures 4A–4C), showing the importance of Shisa7 C-tail in regulating tonic inhibition. We then generated point mutation at S306, S405, or S430, mutating these serine residues to alanine (A), respectively, and expressed them individually in Shisa7 KO hippocampal neurons. Intriguingly, while both Shisa7 S306A and Shisa7 S430A restored tonic current deficits in Shisa7 KO neurons, Shisa7 S405A failed to rescue the reduced tonic currents (Figures 4A–4C), demonstrating that Shisa7 S405 plays a critical role in the regulation of tonic inhibition. Similar results were obtained in overexpression experiments (Figure S3). Specifically, while overexpression of Shisa7 or Shisa7 phosphomimetic (S405D) mutant substantially increased tonic inhibitory currents in WT hippocampal cultures, tonic inhibition was significantly decreased in neurons expressing Shisa7 ΔC or Shisa7 S405A (Figure S3).

What are the mechanisms for the inability of Shisa7 S405A to rescue tonic current deficits in Shisa7 KO neurons? We found that transfection of WT Shisa7 back into Shisa7 KO neurons significantly increased expression levels of surface α5 (Figure 4D). In contrast, expression of Shisa7 S405A did not significantly alter surface α5 expression (Figure 4D), suggesting that S405 is important in the regulation of surface abundance of α5-$GABA_A$Rs. FRAP-FLIP experiments in live hippocampal neurons further showed that Shisa7, but not Shisa7 S405A,

restored the reduced exocytosis of SEP-α5 in Shisa7 KO neurons (Figures 4E and 4F), showing that S405 is crucial for α5-$GABA_AR$ forward trafficking to the neuronal surface. Thus, Shisa7 S405 controls α5-$GABA_AR$ exocytosis, which in turn regulates tonic inhibition.

Homeostatic potentiation of tonic inhibition requires Shisa7 S405

Homeostatic plasticity plays a critical role in regulating synaptic strength and neuronal excitability. Both excitatory and inhibitory synapses have been shown to be capable of undergoing homeostatic regulation in response to chronic changes of neuronal network activity (Hartman et al., 2006; Kilman et al., 2002; Turrigiano et al., 1998; Turrigiano and Nelson, 2004). However, it remains unclear whether tonic inhibition can also undergo homeostatic plasticity induced by chronic activity manipulation. To this end, we applied tetrodotoxin (TTX) to block action potentials or used a $GABA_AR$ competitive antagonist, BIC, to chronically reduce or increase neuronal activity, respectively, in hippocampal cultures and then measured tonic inhibition. We found that in WT neuronal cultures, TTX strongly decreased and BIC significantly increased tonic inhibitory currents (Figure 5A), demonstrating bidirectional plasticity of tonic inhibitory currents in response to chronic change of neuronal activity. Strikingly, in Shisa7 KO hippocampal cultures, while TTX treatment substantially depressed tonic currents, BIC did not significantly alter tonic inhibition (Figure 5A), indicating that Shisa7 is critical for homeostatic potentiation of tonic inhibition in hippocampal neurons. Application of L-655,708 to block α5-$GABA_ARs$ revealed that BIC-induced potentiation of tonic currents was largely mediated by α5-$GABA_ARs$ (Figure S4). In addition to measuring tonic currents, we performed immunocytochemical assays to determine the abundance of surface α5-$GABA_ARs$ on hippocampal neurons treated with TTX or BIC. We found that TTX treatment substantially reduced surface abundance of α5-$GABA_ARs$ in both WT and Shisa7 KO cultures (Figure 5B). In contrast, although BIC treatment increased surface abundance of α5-$GABA_ARs$ in WT cultures, it failed to induce upregulation of surface α5-$GABA_ARs$ in Shisa7 KO cultures (Figure 5B).

To determine whether the requirement of Shisa7 in the homeostatic upregulation of tonic inhibition observed in neuronal cultures also occurs *in vivo*, we pharmacologically increased neuronal activity in live mice and then recorded tonic inhibitory currents in CA1 neurons in acute hippocampal slices (Figures 5C and 5E). We found that intraperitoneal (i.p.) injection of kainic acid (KA), which stimulates glutamate receptor activity, or pentylenetetrazol (PTZ), which noncompetitively inhibits $GABA_AR$ activity, significantly increased tonic inhibition in WT mice (Figures 5D and 5F). Significantly, neither KA nor PTZ altered tonic inhibitory currents in CA1 neurons in hippocampal slices prepared from Shisa7 KO mice (Figures 5D and 5F). Taken together, Shisa7 is important for the homeostatic potentiation of tonic inhibition both *in vitro* and *in vivo*.

We have shown that PKA and Shisa7 S405 play a critical role in regulating tonic inhibition and α5-$GABA_AR$ exocytosis (Figures 3A, 4E, and 4F). Thus, it is possible that homeostatic potentiation of tonic inhibition induced by BIC treatment would be impaired in neurons treated with PKA inhibitors or expressing Shisa7 S405A mutant. To test this, we first treated

WT hippocampal cultures with BIC and H89, a PKA inhibitor, and measured tonic inhibition (Figure 6A). We found that while BIC treatment on its own induced homeostatic potentiation of tonic inhibition, co-application of BIC and H89 abolished the upregulation of tonic currents (Figure 6B), indicating that BIC-induced increase of tonic inhibition requires PKA activity. We also expressed Shisa7 S405A mutant in hippocampal cultures and measured homeostatic upregulation of tonic inhibitory currents (Figure 6C). Similar to the data shown in Figure 5A, BIC treatment substantially increased tonic currents in control neurons (Figure 6D). However, in neurons expressing the Shisa7 S405A mutant, BIC treatment did not significantly induce homeostatic enhancement of tonic inhibition (Figure 6D). Thus, Shisa7 S405, a phosphorylation substrate of PKA, plays an important role in α5-$GABA_AR$ exocytosis as well as is critical for homeostatic upregulation of tonic inhibition.

Tonic inhibition changes over the daily sleep/wake cycle in a Shisa7-dependent manner

We have shown that tonic inhibition can be dynamically regulated by neuronal activity and that Shisa7 S405 plays a critical role in the regulation of homeostatic plasticity of tonic inhibition induced by chronic activity manipulation. We thus wondered whether homeostatic adaptation of tonic inhibition could be driven by behavioral states *in vivo*, such as sleep, as a number of homeostatic processes in the brain have been reported to be associated with the sleep/wake cycle (Cirelli, 2017; Tononi and Cirelli, 2014). To this end, we employed a PiezoSleep mouse behavioral tracking system to monitor sleep/wake cycles in young adult mice (6–8 weeks old) (Figure S5) and performed electrophysiological recordings to measure tonic inhibitory currents in hippocampal CA1 neurons in mice at sleep or wake states (Figures 7A and S5). We noticed that tonic currents in WT young adult mice were much smaller than those recorded in P16–P21 juvenile mice and that there was no significant difference of tonic inhibition in hippocampal CA1 neurons between young adult WT and Shisa7 KO mice (Figures 1B, 7D, and S6C). Application of L655,708, the α5-$GABA_AR$ inverse agonist, revealed that the L655,708-sensitive, α5-$GABA_AR$-mediated component of tonic currents in WT CA1 neurons was substantially reduced in young adult mice (6–8 weeks old), whereas the L655,708-insensitive portion did not change compared with juvenile mice between 2 and 3 weeks old (Figures S6D–S6F). Thus, in young adult mice, there was no significant difference of tonic inhibition between WT and Shisa7 KO CA1 neurons, largely due to decreased α5-$GABA_AR$-mediated tonic currents in WT neurons.

We found that in young adult WT mice, tonic inhibitory currents in hippocampal CA1 neurons changed over the 24-h sleep/wake cycle. Indeed, tonic inhibition was significantly higher in the animals that were awake compared to those asleep (Figure 7B). Strikingly, in Shisa7 KO CA1 neurons, there was no significant change of tonic currents over the daily sleep/wake cycle, and the tonic currents in Shisa7 KO neurons in either sleep or wake states were similar to those in WT mice in the sleep state (Figure 7B). Thus, Shisa7 KO disrupts the increase of tonic inhibition associated with the wake phase.

We also employed sleep deprivation (SD) to manipulate the daily sleep/wake cycle and measured the impact of sleep loss on tonic inhibition (Figure 7C). We found that a 6-h SD increased tonic currents in hippocampal CA1 neurons in WT young adult mice, but not in Shisa7 KO mice (Figure 7D). Thus, acute loss of sleep increases tonic inhibition in

hippocampal CA1 neurons. Significantly, the L655,708-sensitive, α5-$GABA_A$R-mediated component, but not the L655,708-insensitive component, of tonic currents was potentiated by SD in WT, but not Shisa7 KO, mice (Figures S6A and S6B), highlighting that SD-induced increases in tonic inhibition are α5 specific.

We have shown that Shisa7 S405 is critical for α5-$GABA_A$R exocytosis and homeostatic upregulation of tonic inhibition in response to chronically elevated activity (Figures 4 and 6D). Therefore, we examined the role of Shisa7 S405 in SD-induced enhancement of tonic inhibition. MS analysis showed that SD increased expression levels of phosphorylated Shisa7 at S405 in the hippocampus (Figure S7). We then recorded tonic inhibitory currents in hippocampal CA1 neurons prepared from young adult mice that were *in utero* electroporated with Shisa7 S405A mutant (Figures 7E and 7F). We found that overexpression of Shisa7 S405A did not change tonic inhibition (Figure 7G), consistent with the data that the basal tonic inhibition in young adult mice does not depend on Shisa7 (Figures 7D). However, SD-induced potentiation of tonic inhibition was abolished in neurons expressing Shisa7 S405A (Figure 7G), indicating that Shisa7 S405 is required for the new insertion of α5-$GABA_A$Rs to the plasma membrane and, subsequently, upregulation of tonic inhibition associated with sleep loss.

DISCUSSION

Tonic inhibition mediated by extrasynaptic $GABA_A$Rs plays a profound role in the regulation of neuronal excitability and brain function. In this study, we have uncovered a Shisa7-dependent molecular mechanism controlling the abundance of extrasynaptic $GABA_A$Rs and tonic inhibition in hippocampus in juvenile mice. Importantly, tonic inhibition is bidirectionally regulated by neuronal activity, a process requiring Shisa7 phosphorylation. Furthermore, the sleep/wake cycle regulates tonic inhibition through a similar molecular pathway involving Shisa7 phosphorylation in young adult mice. Collectively, these data extend our recent work showing the importance of Shisa7 in regulating synaptic $GABA_A$Rs and inhibitory transmission (Han et al., 2019; Han et al., 2021), provide mechanistic insights into modulation of tonic inhibition both *in vitro* and *in vivo*, and demonstrate a critical molecular link between sleep and tonic inhibition.

Shisa7 and α5-$GABA_A$R-mediated tonic inhibition

In hippocampal CA1 pyramidal neurons, the majority of tonic inhibition is mediated by α5-$GABA_A$Rs that are largely distributed at extrasynaptic membranes (Caraiscos et al., 2004; Glykys et al., 2008; Jacob, 2019). Thus, understanding the mechanisms controlling the abundance of α5-$GABA_A$Rs at the cell surface will be critical for determining how tonic inhibition is dynamically regulated. Our data show that Shisa7 interacts with α5-$GABA_A$Rs and promotes α5-$GABA_A$R trafficking to the cell surface. Indeed, in heterologous cells, co-expression of Shisa7 promotes surface and total expression of α5-$GABA_A$Rs. In hippocampal neurons, overexpression of Shisa7 increases the surface abundance of α5-$GABA_A$Rs and potentiates tonic inhibitory currents. Conversely, in Shisa7 KO hippocampal neurons, surface and total α5-$GABA_A$Rs as well as tonic inhibition are significantly decreased. Mechanistically, Shisa7 plays a critical role in α5-$GABA_A$R exocytosis, but not

endocytosis, in cultured hippocampal neurons. Additionally, Shisa7 regulation of total expression of α5-$GABA_A$Rs in both heterologous cells and in neurons indicates that Shisa7 is critical for α5-$GABA_A$R stability in cells. It is also worth noting that in hippocampal lysates, both α4 and δ subunits do not associate with Shisa7, demonstrating the specificity of Shisa7 with α5-$GABA_A$Rs. Similarly, in Shisa7 KO hippocampal neurons, tonic inhibitory currents mediated by α4δ-$GABA_A$Rs are not altered, suggesting a Shisa7-independent pathway for the regulation of trafficking of these extrasynaptic $GABA_A$Rs. Together, these data reveal a key molecular pathway for the regulation of tonic inhibition and underscore the importance of Shisa7-dependent modulation of both synaptic and extrasynaptic $GABA_A$Rs (Han et al., 2019).

Although the molecular mechanisms underlying the regulation of α5-$GABA_A$R trafficking in neurons are not fully understood, recent studies have identified a number of proteins that interact with the α5 subunit to regulate subcellular targeting. For example, it has been shown that radixin, a cytoskeletal protein linking actin to the plasma membrane, interacts with α5-$GABA_A$Rs and regulates α5-$GABA_A$R clustering at the extrasynaptic membrane (Hausrat et al., 2015; Loebrich et al., 2006). However, radixin is not required for α5-$GABA_A$Rs trafficking to the cell surface, and thus, in radixin KO hippocampal neurons, α5-$GABA_A$R clustering is lost, but tonic inhibition is not altered (Hausrat et al., 2015). In addition, gephyrin interaction with α5-$GABA_A$Rs is important for synaptic localization of the receptors (Brady and Jacob, 2015). A recent study has identified a transmembrane protein, cleft lip and palate transmembrane protein 1 (Clptm1), that interacts with both synaptic and extrasynaptic $GABA_A$Rs and negatively regulates inhibitory transmission and tonic inhibition through trapping the receptors in the endoplasmic reticulum (ER) and Golgi apparatus (Ge et al., 2018). However, Clptm1 interaction with extrasynaptic $GABA_A$Rs lacks subunit specificity, binding to α4, α5, and δ subunits (Ge et al., 2018). It has also been reported that glycine receptors interact with α5-$GABA_A$Rs and regulate α5-$GABA_A$R-mediated currents in both heterologous cells and neurons in the hypoglossal nucleus (Zou et al., 2019). Currently, how Shisa7 functionally interacts with these molecular pathways for the regulation of α5-$GABA_A$R-mediated tonic inhibition remains unknown. Future investigation of α5-$GABA_A$R trafficking in the context of α5-$GABA_A$R native complexes with different binding molecules will provide additional insight into the regulation of tonic inhibition.

A number of studies have shown that protein kinases modulate inhibitory tonic currents in different types of neurons, typically through direct phosphorylation of $GABA_A$R subunits (Connelly et al., 2013; Nakamura et al., 2015). For α5-$GABA_A$R-mediated tonic inhibition, a previous study has shown that CaMKII activity is required for surface expression of α5β3-containing $GABA_A$Rs through phosphorylation of β3 S383 (Saliba et al., 2012). The regulation of tonic inhibition by PKC has also been well documented, especially for α4δ-containing $GABA_A$Rs (Abramian et al., 2010, 2014; Bright and Smart, 2013b; Choi et al., 2008). However, the role of PKC in α5-$GABA_A$R-mediated tonic currents is less clear. It has been reported that stimulation of PKC does not change surface expression of α5 in hippocampal neurons (Abramian et al., 2014), although whether inhibition of PKC activity would alter α5-$GABA_A$R-mediated tonic inhibition was unknown. The role of PKA in tonic inhibition mediated by α5-$GABA_A$Rs appears to be cell-type specific in different

populations of striatal medium spiny neurons, and the mechanisms underlying the regulation of tonic inhibition by PKA remain largely unclear (Janssen et al., 2009). Our data have now shown that blockade of PKA, PKC, or CaMKII activity leads to a significant reduction of tonic inhibitory currents in WT hippocampal neurons. Intriguingly, Shisa7 KO abolishes the effects of pharmacological inhibition of PKA or PKC, but not CaMKII, activities on tonic inhibition, indicating that Shisa7 mediates the regulatory action of PKA or PKC on tonic inhibition. We have also identified two resides, S405 and S430, in the Shisa7 C terminus that can be phosphorylated by PKA. Significantly, Shisa7 S405 is crucial for α5-$GABA_AR$ exocytosis, highlighting a post-translational switch in Shisa7 that is important for regulation of tonic inhibition. Finally, although we have shown the importance of PKC in Shisa7 regulation of tonic inhibition in hippocampal neurons, the mechanisms underlying PKC function remain to be determined.

Shisa7 and activity-dependent homeostatic plasticity of tonic inhibition

Chronic pharmacological manipulation of neuronal activity can induce homeostatic adaptations of excitatory and inhibitory transmission, which are powerful mechanisms controlling neuronal excitability and neural network function (Turrigiano, 2012). However, homeostatic plasticity of tonic inhibition is much less investigated. Our data have shown that tonic inhibition in hippocampal neurons exhibits classic homeostatic plasticity. Indeed, a chronic increase or decrease of neuronal activity by BIC or TTX, respectively, triggers activity-dependent bidirectional regulation of α5-$GABA_AR$ expression at the neuronal surface and tonic inhibition. Importantly, homeostatic upregulation, but not downregulation, of tonic inhibition requires PKA and Shisa7 S405, indicating that Shisa7 S405-dependent α5-$GABA_AR$ exocytosis underlies homeostatic potentiation of tonic inhibition in response to a chronic, global increase of neural activity. In addition, a pharmacological increase of neural activity *in vivo* significantly enhances tonic inhibition in hippocampal CA1 neurons in WT, but not in Shisa7 KO, mice, showing that Shisa7-dependent homeostatic upregulation of tonic inhibition operates both *in vitro* and *in vivo*. Thus, Shisa7 is not only important for maintenance of basal tonic inhibitory currents but also critical for activity-dependent regulation of tonic inhibition in hippocampal neurons. Collectively, our data demonstrate a powerful Shisa7-dependent homeostatic mechanism regulating tonic inhibition that contributes to maintaining a normal range of neuronal excitability in response to chronic changes in neural network activity.

Alternatively, acute changes in neuronal activity within minutes have been shown to regulate α5-$GABA_AR$ abundance at the cell surface and tonic inhibition through a pathway involving calcium influx through L-type calcium channels and subsequent CaMKII activation (Saliba et al., 2012). In this scenario, CaMKII activation leads to phosphorylation at β3 S383, promoting surface insertion of α5β3-containing receptors and enhancing tonic inhibitory currents in hippocampal neurons (Saliba et al., 2012). In agreement, our study has also shown an important role of CaMKII in regulating tonic inhibition. Interestingly, however, our data demonstrate that CaMKII regulation of tonic inhibition operates in a Shisa7-independent manner, whereas homeostatic upregulation of α5 surface expression and tonic inhibition in response to chronic increases in activity require Shisa7, and more specifically, Shisa7 S405, a PKA substrate. Thus, chronic change of neuronal activity triggers a

molecular pathway requiring Shisa7 and PKA, whereas acute manipulation of neuronal activity engages a distinct signaling pathway dependent on CaMKII and β3 phosphorylation. Together, these data reveal discrete signaling mechanisms in hippocampal neurons regulating tonic inhibition in both an activity-dependent and temporal-specific manner.

Shisa7 and regulation of tonic inhibition by sleep

Accumulating evidence has supported the importance of tonic inhibition in regulating a variety of brain functions, including sensory processing (Chadderton et al., 2004; Duguid et al., 2012), motor coordination (Clarkson et al., 2010; Egawa et al., 2012; Woo et al., 2018), and learning and memory (Collinson et al., 2002; Shen et al., 2010; Wang et al., 2012; Wu et al., 2014; Zurek et al., 2014). Dysregulation of tonic inhibition has also been implicated in a number of neurodegenerative and neurodevelopmental disorders (Brickley and Mody, 2012; Glykys and Mody, 2007; Jacob, 2019; Martin et al., 2009; Mohamad and Has, 2019). However, the molecular mechanisms underlying the regulation of tonic inhibition in the context of animal behavior remain largely unknown. On the other hand, sleep is a fundamental physiological process essential for normal brain functioning in animals. It has been proposed that during the daily sleep/wake cycle, homeostatic plasticity of synaptic connections and neuronal excitability occur and play crucial roles in learning and memory (Cirelli, 2017; de Vivo et al., 2017; Diering et al., 2017; Hengen et al., 2016; Tononi and Cirelli, 2014). However, how tonic inhibition is involved in and regulated by the sleep/wake cycle remains unclear. Answers to these questions will not only provide insight into the molecular pathways regulated by sleep but also offer potential specific therapeutic targets for the treatment of sleep disorders.

Our data show that tonic inhibition in hippocampal CA1 neurons is dynamically modulated during the daily sleep/wake cycle. Specifically, tonic inhibition mediated by α5-$GABA_A$Rs in wake is significantly higher than that in sleep. Importantly, the increase of tonic inhibition in the wake state is abolished in Shisa7 KO mice, and SD enhances tonic inhibition in WT, but not in Shisa7 KO, mice. Thus, the upregulation of tonic inhibition in CA1 neurons associated with the wake state requires Shisa7. Furthermore, Shisa7 S405 is critical for potentiation of tonic inhibition induced by SD, indicating that Shisa7 S405-dependent exocytosis of α5-$GABA_A$Rs underlies upregulation of tonic inhibition in CA1 neurons during the wake state.

We noticed that in young adult mice (6–8 weeks old), tonic inhibitory currents in hippocampal CA1 neurons were smaller than that in juvenile mice between 2 and 3 weeks old. A similar change of tonic inhibition during development has previously been reported (Al-Muhtasib et al., 2018; Chudomel et al., 2015; Holter et al., 2010; Pandit et al., 2017). Our data indicate that the decrease of tonic inhibition in hippocampal CA1 neurons in WT young adult mice is due to a significant reduction of the component of α5-$GABA_A$R-mediated tonic currents. Therefore, it is plausible that the diminished contribution of α5-$GABA_A$Rs to tonic inhibition in hippocampal CA1 neurons in young adult mice might account for the little change of tonic inhibition in Shisa7 KO mice at this developmental stage. Intriguingly, enhancement of tonic inhibition in the wake phase or induced by SD in young adult mice requires Shisa7-mediated insertion of α5-$GABA_A$Rs, suggesting that

although Shisa7 is not necessary for the basal tonic inhibition, it is critical for activity-dependent α5-$GABA_A$R trafficking and upregulation of tonic inhibition. Future experiments examining the mechanisms underlying Shisa7 independent regulation of α5-$GABA_A$R-mediated basal tonic inhibition in young adult mice will provide additional insight into dynamic regulation of tonic inhibition *in vivo*.

A recent study has reported that inhibitory transmission changes over the daily sleep/wake cycle. Specifically, in hippocampal CA1 and cortical pyramidal neurons synaptic inhibition is increased, whereas synaptic excitation is decreased, leading to altered excitation/inhibition balance during the sleep phase (Bridi et al., 2019). Thus, it appears that different molecular and cellular mechanisms exist in neurons governing the regulation of inhibitory synaptic transmission and tonic inhibition over the daily sleep/wake cycle. Currently, the functional significance of increase of tonic inhibition in wake remains to be determined. It has been reported that tonic inhibition helps set the threshold for the induction of long-term potentiation at excitatory synapses (Martin et al., 2010) and thus may enhance selectivity during learning in wake (Tononi and Cirelli, 2014). Interestingly, tonic inhibition has also been shown to be dynamically modulated by a variety of physiological and pathological processes *in vivo*, including learning, puberty, the ovarian cycle, pregnancy, epilepsy, and acute stress (Cushman et al., 2014; Maguire and Mody, 2008; Maguire et al., 2005; Peng et al., 2004; Serra et al., 2006; Shen et al., 2007, 2010; Zhang et al., 2007), indicating that plasticity of tonic inhibition is broadly implicated in animal behavior and cognition. However, the role of Shisa7 in the dynamic regulation of tonic inhibition triggered by these behavioral and cognitive processes remains to be determined.

In summary, we have uncovered a critical role of Shisa7 in the regulation of α5-$GABA_A$R exocytosis and tonic inhibition in juvenile mice, identified a molecular pathway controlling activity-dependent modulation of tonic inhibitory currents, and revealed a link between the daily sleep/wake cycle and tonic inhibition regulation in young adult mice. As dysfunctions in tonic inhibition have been implicated in a number of neurological and psychiatric disorders and extrasynaptic $GABA_A$Rs are important drug targets for the treatment of epilepsy, depression, and cognitive impairment (Brickley and Mody, 2012; Glykys and Mody, 2007; Jacob, 2019; Martin et al., 2009; Mohamad and Has, 2019), our findings also provide insight to design therapeutic reagents for intervening and treating brain disorders.

Limitations of study

Finally, caution should be taken in the interpretation of the regulation of tonic inhibition by the daily sleep/wake cycle. Although we have defined sleep and wake using a PiezoSleep behavioral tracking system, our approach to measure sleep patterns is indirect and may not fully capture the real-time sleep pattern and duration. In addition, different criteria and approaches have been employed to measure sleep in rodents in the literature (Bridi et al., 2019; de Vivo et al., 2017; Diering et al., 2017; Liu et al., 2010), indicating a need in establishing a well-validated, noninvasive system to rapidly analyze sleep for subsequent electrophysiological or biochemical investigations in the future. Furthermore, we could not completely rule out the potential influence on tonic inhibitory currents by circumstantial factors associated with the *in vitro* preparation of mouse brain slices. Considering these,

while our data show a significant change of tonic currents over the daily sleep/wake cycle, future work toward a more complete understanding of sleep-dependent regulation of tonic inhibition will be necessary and invaluable.

STAR★METHODS

RESOURCE AVAILABILITY

Lead contact—Further information and requests for resources and reagents should be directed to the Lead Contact, Wei Lu (luw4@mail.nih.gov).

Materials availability—All unique reagents generated in this study are available from the Lead Contact with a completed Materials Transfer Agreement.

Data and code availability—This study did not generate datasets/code.

EXPERIMENTAL MODEL AND SUBJECT DETAILS

Animals—All animal handling was performed in accordance with animal protocols approved by the Institutional Animal Care and Use Committee (IACUC) at NIH/NINDS. C57BL/6 mice were purchased from Charles River and Shisa7 germline knockout (KO) mice were generated as described previously (Han et al., 2019). All mice were housed and bred in a conventional vivarium with *ad libitum* access to food and water under a 12-h circadian cycle. Time-pregnant mice at E17.5–18.5 were used for dissociated hippocampal neuronal culture. Time-pregnant mice at E14.5–15.5 were used for in utero electroporation (IUE). Mice of both sexes at P16–21 were used for biochemical experiments. To investigate the effects of Shisa7 KO on tonic inhibition *in vivo*, mice of both sexes at P16–21 were used to prepare acute hippocampal slices for electrophysiology experiments. To evaluate the effects of sleep/wake cycle or sleep deprivation (SD) on tonic inhibition, young adult male mice (6–8 weeks old) were used for electrophysiology experiments.

Cell lines—HEK293T cells (ATCC, Cat# CRL-11268) were maintained with culture media containing 1% penicillin-streptomycin (GIBCO), 10% FBS (GIBCO) in Dulbecco's Modified Eagle's Medium (DMEM, GIBCO), in a humidified incubator at 37°C with 5% CO_2.

Dissociated hippocampal neuronal culture—Mice hippocampal neurons were dissected from E17.5–18.5 wild-type or Shisa7 KO embryos and cultures were prepared as previously described (Han et al., 2019). Briefly, the hippocampi were dissected from embryos of both sexes and digested in Hank's Balanced Salt Solution (HBSS, GIBCO) containing 20 U/ml papain (Worthington) and 100 U/ml DNase I (Worthington) at 37°C for 45 min. After centrifugation for 5 min at 800 rpm, the pellet was resuspended in HBSS containing 100 U/ml DNase I, and was fully dissociated by pipetting up and down. Cells were then transferred into HBSS containing trypsin inhibitor (10 mg/ml, Sigma-Aldrich) and BSA (10 mg/ml, Sigma-Aldrich). After centrifugation for 10 min at 800 rpm, cells were resuspended in Neurobasal media (GIBCO) supplemented with 2% B27 (GIBCO) and 2 mM GlutaMAX (GIBCO) and were plated on poly-D-lysine (Sigma-Aldrich)-coated glass

coverslips residing in 24-well plates at a density of 1.5×10^5 cells/well for electrophysiology experiments or 0.8×10^5 cells/well for imaging experiments. Cultures were maintained in Neurobasal media supplemented with 2% B27 and 2 mM GlutaMAX in a humidified incubator at 37°C with 5% CO_2. Culture media were changed by half volume once a week.

METHOD DETAILS

Plasmids—pCAGGs-Shisa7-IRES-GFP and pcDNA3-Flag-Shisa7 were used as previously described (Han et al., 2019). α5-GFP was purchased from Addgene (plasmid # 118956). Human $GABA_AR$ α5, β3 and γ2 in pcDNA3.1 Zeo were gifts from Joseph Lynch's lab at University of Queensland, Australia. The coding sequence of Shisa7 phosphomimic (S405D), phosphodeficient (S306A, S405A, S430A), and ΔC-tail mutants were generated separately by overlapping PCR using pcDNA3-Flag-Shisa7 as a template and were then inserted into the pCAGGs-IRES-GFP or pCAGGs-IRES-mCherry vectors. The coding sequence of Superecliptic pHluorin (SEP)-tagged α5 was obtained by PCR with Human $GABA_AR$ α5 as the template and then replaced α1 coding sequenceinSEP-α1 (Addgene plasmid # 49168). pGEX-4T-Shisa7 (211–349) and pGEX-4T-Shisa7 (347–558) were generated by GenScript. All plasmids were confirmed by DNA sequencing.

Cell transfection—HEK293T cells were transfected with α5β3γ2 receptors, together with GFP or Shisa7/GFP, using CalPhos Mammalian Transfection Kit (Takara). Electrophysiological recordings or immunostaining were performed 24–48 h after transfection. Hippocampal neurons at DIV13–15 were transfected with SEP-α5 using Lipofectamine 3000 (Thermo Fisher Scientific) and live imaging was performed 24 h after transfection. Hippocampal neurons at DIV16 were transfected with Shisa7 phosphomimic (S405D), phosphodeficient (S306A, S405A, S430A) or ΔC-tail mutants for overexpression and rescue experiments using NeuroMag reagent (Oz Biosciences). Electrophysiological recordings or immunostaining were performed 36–72 h after transfection. All transfection kits were used according to the manufacturer's instructions.

Immunocytochemistry—Transfected HEK293T cells and hippocampal neurons grown on glass coverslips were fixed with 4% paraformaldehyde and 4% sucrose in PBS. For surface α5 staining, cells were blocked with 10% NGS, washed, and incubated with rabbit α5 antibody (1:500, Synaptic Systems) in 3% NGS overnight at 4°C, and then washed, and incubated with Alexa 555-conjugated anti-rabbit secondary antibody (1:1000, Thermo Fisher Scientific) in 3% NGS for 1 h. After surface staining, cells were permeabilized with 0.25% Triton X-100 for 15 min, washed, blocked in 10% NGS, and then incubated with mouse α5 antibody (1:500, James Trimmer, University of California at Davis), mouse gephyrin antibody (1:500, Synaptic Systems) or chicken MAP2 antibody (1:1000, Aves Labs) in 3% NGS overnight at 4°C. Cells were then washed, and incubated with Alexa 488-conjugated anti-mouse secondary antibody (1:1000, Jackson ImmunoResearch Labs) or Alexa 647-conjugated anti-chicken secondary antibody (1:1000, Thermo Fisher Scientific) in 3% NGS for 1 h. Coverslips were then washed for three times with PBS and mounted with Fluoromount-G (Southern Biotech).

For the endocytosis assay, hippocampal neurons at DIV16 were incubated live with rabbit α5 antibody (1:500, Synaptic Systems) at 37°C for 10 min in conditioned culture medium. After incubation, the neurons were washed with PBS and then incubated in antibody-free medium to allow antibody-bound receptors to undergo internalization at 37°C for 30 min, followed by fixation with 4% paraformaldehyde and 4% sucrose in PBS. After fixation, neurons were washed and then blocked with 10% NGS for 1 h, exposed to Alexa 555-conjugated anti-rabbit secondary antibody (1:200, Thermo Fisher Scientific) for 1 h under the nonpermeabilized condition, and then internalized α5 was labeled with Alexa 488-conjugated anti-rabbit secondary antibody (1:1000, Jackson ImmunoResearch Labs) for 1 h after permeabilization in PBS containing 0.25% Triton X-100 and blocking in 10% NGS. Coverslips were washed for three times with PBS and mounted with Fluoromount-G.

Image acquisition—For Immunocytochemistry in fixed neurons, fluorescence images were acquired on a Zeiss LSM 880 laser scanning confocal microscope with a 63 × 1.4 NA oil immersion objective. Multiple z sections (4–5 optical slices) were collected with step intervals of 0.39 μm in the z direction. Scan speed function were set to 9 and the mean of four lines was collected. Images were captured using a 1024 × 1024 pixel screen for HEK293T cells and a 1024 × 256 pixel screen for neuronal dendrites. All the parameters used in confocal microscopy were consistent in each experiment, including the laser excitation power, detector, off-set gains, and the pinhole diameter.

Live imaging with FRAP-FLIP—For live imaging of α5 receptor exocytosis, fluorescence recovery after photobleaching (FRAP) and fluorescence loss in photobleaching (FLIP) were applied as previously described with minor modifications (Hildick et al., 2012; Nakahata et al., 2017). Briefly, hippocampal neurons at DIV13–15 were transfected with SEP-α5 (and mCherry, Shisa7/mCherry or Shisa7 S405A/mCherry) constructs for 24 h prior to experiments. Fluorescence of SEP-α5 was photobleached using a 488 nm laser (200 mW) at 80% power in a rectangular region of dendrites expressing SEP-α5. Then, repetitive photobleaching (10% laser power) at the edge of the initial photobleaching region was applied throughout the imaging period panel in order to avoid the lateral diffusion of nonbleached surface receptors. FRAP of SEP-α5 in the central region was used to measure receptor exocytosis. Recovery from photobleaching in the central region was monitored by consecutive acquisitions every 30 s for 7 min and normalized to the fluorescence measured before photobleaching.

Co-immunoprecipitation and western blot—Transfected HEK293T cells were homogenized in ice-cold lysis buffer containing 25 mM Tris pH 7.5, 1% Triton X-100, 150 mM NaCl, 5% glycerol, 1 mM EDTA and protease inhibitor cocktail (Roche). After incubation on ice for 30 min, the homogenates were centrifuged at 12,000 g at 4°C for 15 min. The supernatants were collected, and the total protein concentrations were measured using BCA Protein Assay Kit (Thermo Fisher Scientific). For immunoprecipitation, the supernatants were incubated with 40 μL Anti-FLAG M2 Affinity gel (Sigma-Aldrich) at 4°C overnight. The beads were collected by centrifugation and washed three times with lysis buffer. The precipitated proteins were eluted with SDS loading buffer with β-mercaptoethanol, and denatured at 37°C for 10 min before SDS-PAGE and immunoblotting.

For brain tissue lysate immunoprecipitation, hippocampi from P16–21 mice were dissected and homogenized in ice-cold lysis buffer as mentioned above with phosphatase inhibitor cocktail (Thermo Fisher Scientific). The insoluble debris was removed by centrifugation at 12,000 g for 15 min. Hippocampal lysates were incubated with a custom-made anti-Shisa7 polyclonal antibody (1:500, GenScript; Han et al., 2019) at 4°C overnight. Dynabead Protein G (Thermo Fisher Scientific) was then added to the mixture and incubated for 2 h. The beads were washed three times with lysis buffer. The protein samples were then eluted with SDS loading buffer with β-mercaptoethanol and denatured at 37°C for 10 min. The denatured samples were resolved by SDS-PAGE and analyzed by Mass Spectrometry or immunoblotting.

For western blot, the proteins were resolved by SDS-PAGE and then transferred onto PVDF membranes. The membranes were blocked, incubated with primary antibodies at 4°C overnight, washed and incubated with HRP-conjugated secondary antibodies for 1 h at room temperature (~23°C). Protein was detected with the standard enhanced chemiluminescence (ECL) method, and documented by a gel imaging system (Li-COR Odyssey).

GST fusion protein production and *in vitro* phosphorylation—The Shisa7 C-terminal domains (amino acids 211–349 and 347–558, respectively) were cloned into pGEX-4T. GST fusion proteins were produced in the BL21 *E. coli* strain (Thermo Fisher Scientific) by inducing protein production with 50 μM isopropyl β-d-1-thio-galactopyranoside (IPTG) at 16°C for 10–12 h. *E. coli* were then lysed with a sonicator in a Tris-buffered saline (TBS) buffer containing protease inhibitors (Roche), 100 μg/ml lysozyme, 1 mM dithiothreitol (DTT) and 0.2 mM EDTA. The fusion proteins were purified using Pierce Glutathione Agarose (Thermo Fisher Scientific) according to manufacturer's instructions. For PKA *in vitro* phosphorylation, the fusion proteins were phosphorylated in PKA kinase buffer (10 mM HEPES, 20 mM $MgCl_2$, and 50 μM ATP) with 50 ng of purified PKA catalytic subunit (Promega). For PKC *in vitro* phosphorylation, reactions were performed in PKC kinase buffer (20 mM HEPES, pH 7.4, 1.67 mM $CaCl_2$, 1 mM DTT, 10 mM $MgCl_2$, and 50 μM ATP) with 10 ng of purified PKC (Promega). All *in vitro* kinase assays were performed at 30°C for 30 min. The reactions were halted with addition of SDS loading buffer with β-mercaptoethanol and incubation at 65°C for 5 min. The proteins were resolved by SDS-PAGE and then were stained with Coomassie blue. Coomassie staining gel were cut out and were analyzed by Mass Spectrometry.

Mass spectrometry analysis—Protein samples were reduced with 5 mM TECP, followed by 5 mM NEM treatment, and digested with trypsin. Digests were used for LC-MS/MS data acquisition on an Orbitrap Lumos mass spectrometer (Thermo Fisher Scientific) coupled with a 3000 Ultimate HPLC instrument (Thermo Fisher Scientific). Peptides were separated using an ES803 column (Thermo Fisher Scientific) with the percentage of mobile phase B (MPB, which contains 98% ACN, 1.9% H_2O, 0.1% FA) increased from 2% to 24% in 38 or 64 min. The LC-MS/MS data were acquired in data-dependent mode with a decision tree method. The MS resolution is 120K at m/z 400, MS scan range is 300–1500 m/z, the automated gain control (AGC) target is 2×10^5. The quadrupole isolation window is 1.6 m/z. Precursors with charge states 2–6 and intensity

higher than 1×10^4 within a 3-s cycle between MS1 scans were selected for MS/MS acquisition in the linear ion trap. Mascot database search was performed for PTM analysis. The following parameters were used for samples digested with trypsin: 2 missed cleavages allowed; N-ethylmaleimide on cysteines as fixed modification; oxidation (M) and phosphorylation (STY) as variable modification, the mass tolerance was set at 10 ppm for precursor ions and 0.6 Da for fragment ions. Phosphorylated peptides matched by Mascot search were manually curated. The label-free quantitation analysis was performed using Proteome Discoverer 2.4 software. The abundance values of each phosphopeptide were scaled so that the average abundance was one in each experiment. Then, the scaled data for the same phosphopeptide were integrated together for analysis.

Electrophysiology—For GABA-evoked whole-cell currents, HEK293T cells were co-transfected with α5β3γ2 receptors, together with either GFP or Shisa7/GFP plasmids. All recordings were performed after 24–48 h transfection. Coverslips containing HEK293T cells were perfused continuously with anexternal solution (in mM): 140NaCl, 5 KCl, 2 $CaCl_2$, 1 $MgCl_2$, 10HEPES and 10D-glucose. The internal solution contained (in mM): 70 $CsMeSO_4$, 70 CsCl, 8 NaCl, 10 HEPES, 0.3 Na-GTP, 4 Mg-ATP and 0.3 EGTA (pH 7.3; osmolality 285–290 mOsm). Experiments were started 3–5 min after achieving the whole-cell configuration at −70 mV. Rapid application/removal of saturating GABA (10 mM) was performed using a computer-controlled multi-barrel perfusion system (Automate Scientific). For recording in dissociated hippocampal cultures, neurons growing on coverslips were transferred to a submersion chamber, perfused with artificial cerebrospinal fluid (ACSF) containing (in mM): 130 NaCl, 3.5 KCl, 24 $NaHCO_3$, 1.25 NaH_2PO_4-H_2O, 10 glucose, 2.5 $CaCl_2$ and 1.5 $MgCl_2$ supplemented with 0.5 μM TTX (Alomone Labs), 20 μM DNQX (Alomone labs) and 50 μM D-APV (Abcam) without exogenous GABA. The intracellular solution contained (in mM) 70 $CsMeSO_4$, 70 CsCl, 8 NaCl, 10 HEPES, 0.3 Na-GTP, 4 Mg-ATP, and 0.3 EGTA (pH 7.3; osmolality 285–290 mOsm). In some recordings as indicated, H89 (20 μM, Abcam), GF 109203X (200 nM, Abcam) or KN62 (3 μM, Abcam) was added directly into intracellular solution to inhibit PKA, PKC or CaMKII, respectively via intra-pipette administration. To induce homeostatic plasticity *in vitro*, neurons were treated with 1 μM TTX or 40 μM bicuculline for 48 h prior to electrophysiological recording. For recording in acute brain slices, transverse hippocampal slices (300 μm thickness) were prepared from 16–21 days old mice of both sexes or 6–8 weeks old male mice in chilled high sucrose cutting solution, containing (in mM): 2.5 KCl, 0.5 $CaCl_2$, 7 $MgCl_2$, 1.25 NaH_2PO_4, 25 $NaHCO_3$, 7 glucose, 210 sucrose and 1.3 ascorbic acid. All mice were anesthetized by isoflurane (~15 s), and then the brain was rapidly removed for slicing. We do not expect that the anesthesia will have any effect on tonic inhibition as it is only applied for a few seconds. The slices were recovered in ACSF at 32°C for 30 min and then were incubated for an additional 30 min in ACSF at room temperature. To record tonic currents, slices were transferred to a submersion chamber, perfused with ACSF with 20 μM DNQX, 50 μM D-APV and 5 μM GABA. We recognize that in the literature, tonic GABA currents have been recorded under conditions of added GABA or without exogenous GABA, depending on the experimental preparations (Bright and Smart, 2013a; Glykys and Mody, 2007). In dentate gyrus granule cells and dLGN thalamic relay neurons in acute brain slices where tonic GABAergic inhibition can be recorded without the need of adding GABA to the

ACSF (Bright and Smart, 2013b). In CA1 pyramidal neurons in acute hippocampal slices, ACSF supplemented with 5 μM GABA has also been used for tonic current recording (Glykys et al., 2008; Wang et al., 2012). Under our experimental conditions, only negligible currents in CA1 pyramidal neurons can be recorded in acute hippocampal slices without added GABA. Thus, 5 μM GABA was added in the ACSF in all experiments recording tonic currents in hippocampal CA1 neurons in acute hippocampal slices. The intracellular solution contained (in mM) 130 CsCl, 8.5 NaCl, 5 HEPES, 4 $MgCl_2$, 4 Na-ATP, 0.3 Na-GTP and 1 QX-314 (pH 7.3; osmolality 285–290 mOsm). To induce activity elevation *in vivo*, mice at P16 were intraperitoneally injected with kainic acid (KA, 4 mg/kg), pentylenetetrazol (PTZ, 40 mg/kg) or as control, an equal volume of saline. Hippocampal CA1 pyramidal cells were recorded 6 h after KA injection or 24 h after PTZ injection. The experimenters were not blinded to the genotype or the treatment groups.

To measure tonic inhibitory currents in neuronal cultures or in acute hippocampal slices, the $GABA_AR$ competitive antagonist bicuculline (20 μM, Abcam) was bath applied after obtaining a stable baseline recording at a holding potential of −70 mV. Custom-written macros running under Igor Pro (WaveMetrics) were used to determine the values of tonic currents. An all-points histogram was plotted for a 20-s period before and during bath-application of bicuculline, fitting the histogram with a Gaussian distribution gave the mean baseline holding currents, and the difference in baseline holding currents before and during bicuculline application was calculated to be the tonic currents. In some recordings as indicated, L-655,708 (100 nM, Sigma-Aldrich) or THIP (10 μM, Santa Cruz) was added to the ACSF via perfusion and their effects on tonic currents were recorded. Tonic currents were normalized to membrane capacitance, to account for variability in cell size. Membrane capacitance was obtained using the voltage step method as described previously (Gentet et al., 2000). Series resistance was monitored and not compensated, and cells in which series resistance was more than 25 MΩ or varied by 25% during a recording session were discarded. Whole-cell recordings were obtained from cells visualized with a fixed stage upright microscope (BX51WI, Olympus). Fluorescence-positive cells were identified by epifluorescence microscopy. All recordings were performed at room temperature. Data were collected with a Multiclamp 700B amplifier (Axon Instruments), filtered at 2 kHz, and digitized at 10 kHz.

In utero electroporation—In Utero electroporation was performed as described previously (Li et al., 2017). Briefly, E14.5–15.5 timed-pregnant mice were anesthetized and their uterine horns were exposed with a midline laparotomy incision. Embryos were gently pulled outside the abdominal cavity. A volume of 2 μL of expression constructs Shisa7 S405A/GFP (2 μg/μL) plus 0.05% fast green (Sigma-Aldrich) was injected into the lateral ventricles of the embryonic brain with a glass micropipette. For electroporation, 5 × 50 ms, 45 V square pulses separated by 950 ms intervals were delivered with forceps-type electrodes connected to an ECM 830 electroporator (BTX Harvard Apparatus). The uterus was then returned to the abdominal cavity, and Buprenex (0.1 mg/kg) was applied before the wound was sutured. The pregnant mouse was warmed in an incubator until it became conscious. Ketoprofen (5 mg/kg) was administered daily for two days after surgery.

Piezoelectric sleep recording—Sleep-wake activity was recorded using a piezoelectric monitoring system (Signal Solutions) as described with minor modifications (Holth et al., 2019; Hou et al., 2019; Mang et al., 2014). It has been demonstrated that this sensitive system estimated total sleep time with more than 90% accuracy compared to EEG, although it cannot distinguish rapid eye movement (REM) sleep from non-rapid eye movement (NREM) (Mang et al., 2014). Prior to piezoelectric recording, 6–8 weeks old male mice were singly housed and habituated to the recording cage with free access to food and water for 2 days under a 12-h circadian cycle. During piezoelectric recording, mice were left undisturbed and the piezoelectric signals in 2-s epochs were automatically analyzed by a linear discriminant classifier algorithm and classified as sleep or wake, as detailed in previous studies (Hou et al., 2019; Mang et al., 2014). Total sleep percentages and hourly sleep percentages were calculated using SleepStats Data Explorer (Signal Solutions). Based on the sleep pattern we recorded (Figure S5) and the criteria used in the previous study [73], we defined sleep/wake mice as follows: “sleep mice” were asleep for at least 65% of the previous 4 h (≥60% per hour), whereas “wake mice” were awake for at least 75% of the previous 4 h (≥70% per hour). Mice were selected for electrophysiology experiments only if they met the criteria. For the mice used in all other experiments not related to the sleep/wake behavioral experiments, we didn’t measure their sleep-wake behavior before slicing, and mice were pooled for following experiments.

Sleep deprivation—Mice were sleep-deprived for 6 h by gentle handling starting at the light onset. At the beginning of the sleep deprivation period, mice were taken from their home cages and transferred to a new cage individually and were gently handled (by gentle tapping of the cage, disturbing the bedding materials or gentle prodding mouse with paintbrush) every time they were falling asleep. Sleep deprivation was continued until the end of the sixth hour. As a control, mice were undisturbed during the first 6 h in the light phase. After sleep deprivation, mice were sacrificed and subjected to electrophysiological recording.

QUANTIFICATION AND STATISTICAL ANALYSIS

Image analysis—For fluorescence intensity analysis, maximal projection images were created with LSM880 browser software (Zeiss) from 5–6 serial optical sections. Image analysis was performed using ImageJ (NIH). The fluorescence intensity was determined from fluorescent signal above a threshold set for distinguishing cell morphology from background. For quantification of fluorescence intensity, region-of-interest (ROI) was defined along a segment of the dendrite (30–35 μm), or an entire HEK293T cell. Background intensity was subtracted by measuring a cell-lacking region in each image. The average values of fluorescence intensities in ROI (the total fluorescence intensity divided by the total area of a dendritic segment or a HEK293T cell) were calculated by ImageJ. The average fluorescence intensity in each group was normalized to their control group.

Statistical analysis—For all biochemical, cell biological and electrophysiological recordings, at least three independent experiments were performed (independent cultures, transfections or different mice). Statistical analysis was performed in GraphPad Prism 8.0 software. Normality distribution was tested by the Shapiro-Wilk test before carrying out a

subsequent statistical test. Direct comparisons between two groups were made using two-tailed Student's t test or Mann-Whitney U test. Multiple comparisons were performed using one-way ANOVA, Kruskal-Wallis test or two-way ANOVA with corrections for multiple comparisons test (see figure legends for specifics). For power analysis, G*Power was used to analyze the sample size. The statistical significance was defined as *$p < 0.05$, **$p < 0.01$, ***$p < 0.001$ or ****$p < 0.0001$, respectively. All data are presented as mean ± SEM.

Supplementary Material

Refer to Web version on PubMed Central for supplementary material.

ACKNOWLEDGMENTS

We are grateful to all members of the Lu laboratory for comments on the manuscript. This work was supported by the NIH/NINDS Intramural Research Program (W.L. and Y.L.).

REFERENCES

Abramian AM, Comenencia-Ortiz E, Vithlani M, Tretter EV, Sieghart W, Davies PA, and Moss SJ (2010). Protein kinase C phosphorylation regulates membrane insertion of GABAA receptor subtypes that mediate tonic inhibition. J. Biol. Chem 285, 41795–41805. [PubMed: 20940303]

Abramian AM, Comenencia-Ortiz E, Modgil A, Vien TN, Nakamura Y, Moore YE, Maguire JL, Terunuma M, Davies PA, and Moss SJ (2014). Neurosteroids promote phosphorylation and membrane insertion of extrasynaptic GABAA receptors. Proc. Natl. Acad. Sci. USA 111, 7132–7137. [PubMed: 24778259]

Al-Muhtasib N, Sepulveda-Rodriguez A, Vicini S, and Forcelli PA (2018). Neonatal phenobarbital exposure disrupts GABAergic synaptic maturation in rat CA1 neurons. Epilepsia 59, 333–344. [PubMed: 29315524]

Belelli D, Harrison NL, Maguire J, Macdonald RL, Walker MC, and Cope DW (2009). Extrasynaptic GABAA receptors: form, pharmacology, and function. J. Neurosci 29, 12757–12763. [PubMed: 19828786]

Braat S, and Kooy RF (2015). The GABAA Receptor as a Therapeutic Target for Neurodevelopmental Disorders. Neuron 86, 1119–1130. [PubMed: 26050032]

Brady ML, and Jacob TC (2015). Synaptic localization of α5 GABA (A) receptors via gephyrin interaction regulates dendritic outgrowth and spine maturation. Dev. Neurobiol 75, 1241–1251. [PubMed: 25663431]

Brickley SG, and Mody I (2012). Extrasynaptic GABA(A) receptors: their function in the CNS and implications for disease. Neuron 73, 23–34. [PubMed: 22243744]

Bridi MCD, Zong F-J, Min X, Luo N, Tran T, Qiu J, Severin D, Zhang X-T, Wang G, Zhu Z-J, et al. (2019). Daily Oscillation of the Excitation-Inhibition Balance in Visual Cortical Circuits. Neuron.

Bright DP, and Smart TG (2013a). Methods for recording and measuring tonic GABAA receptor-mediated inhibition. Front. Neural Circuits 7, 193. [PubMed: 24367296]

Bright DP, and Smart TG (2013b). Protein kinase C regulates tonic GABA(A) receptor-mediated inhibition in the hippocampus and thalamus. Eur.J. Neurosci 38, 3408–3423. [PubMed: 24102973]

Brown N, Kerby J, Bonnert TP, Whiting PJ, and Wafford KA (2002). Pharmacological characterization of a novel cell line expressing human alpha(4)beta(3)delta GABA(A) receptors. Br. J. Pharmacol 136, 965–974. [PubMed: 12145096]

Butler KM, Moody OA, Schuler E, Coryell J, Alexander JJ, Jenkins A, and Escayg A (2018). De novo variants in GABRA2 and GABRA5 alter receptor function and contribute to early-onset epilepsy. Brain 141, 2392–2405. [PubMed: 29961870]

Caraiscos VB, Elliott EM, You-Ten KE, Cheng VY, Belelli D, Newell JG, Jackson MF, Lambert JJ, Rosahl TW, Wafford KA, et al. (2004). Tonic inhibition in mouse hippocampal CA1 pyramidal

neurons is mediated by alpha5 subunit-containing gamma-aminobutyric acid type A receptors. Proc. Natl. Acad. Sci. USA 101, 3662–3667. [PubMed: 14993607]

Chadderton P, Margrie TW, and Häusser M (2004). Integration of quanta in cerebellar granule cells during sensory processing. Nature 428, 856–860. [PubMed: 15103377]

Choi DS, Wei W, Deitchman JK, Kharazia VN, Lesscher HM, McMahon T, Wang D, Qi ZH, Sieghart W, Zhang C, et al. (2008). Protein kinase Cdelta regulates ethanol intoxication and enhancement of GABA-stimulated tonic current. J. Neurosci 28, 11890–11899. [PubMed: 19005054]

Chudomel O, Hasson H, Bojar M, Moshé SL, and Galanopoulou AS (2015). Age- and sex-related characteristics of tonic GABA currents in the rat substantia nigra pars reticulata. Neurochem. Res 40, 747–757. [PubMed: 25645446]

Cirelli C (2017). Sleep, synaptic homeostasis and neuronal firing rates. Curr. Opin. Neurobiol 44, 72–79. [PubMed: 28399462]

Clarkson AN, Huang BS, Macisaac SE, Mody I, and Carmichael ST (2010). Reducing excessive GABA-mediated tonic inhibition promotes functional recovery after stroke. Nature 468, 305–309. [PubMed: 21048709]

Collinson N, Kuenzi FM, Jarolimek W, Maubach KA, Cothliff R, Sur C, Smith A, Otu FM, Howell O, Atack JR, et al. (2002). Enhanced learning and memory and altered GABAergic synaptic transmission in mice lacking the alpha 5 subunit of the GABAA receptor. J. Neurosci 22, 5572–5580. [PubMed: 12097508]

Connelly WM, Errington AC, Di Giovanni G, and Crunelli V (2013). Metabotropic regulation of extrasynaptic GABAA receptors. Front. Neural Circuits 7, 171. [PubMed: 24298239]

Cushman JD, Moore MD, Olsen RW, and Fanselow MS (2014). The role of the δ GABA(A) receptor in ovarian cycle-linked changes in hippocampus-dependent learning and memory. Neurochem. Res 39, 1140–1146. [PubMed: 24667980]

de Vivo L, Bellesi M, Marshall W, Bushong EA, Ellisman MH, Tononi G, and Cirelli C (2017). Ultrastructural evidence for synaptic scaling across the wake/sleep cycle. Science 355, 507–510. [PubMed: 28154076]

Diering GH, Nirujogi RS, Roth RH, Worley PF, Pandey A, and Huganir RL (2017). Homer1a drives homeostatic scaling-down of excitatory synapses during sleep. Science 355, 511–515. [PubMed: 28154077]

Duguid I, Branco T, London M, Chadderton P, and Häusser M (2012). Tonic inhibition enhances fidelity of sensory information transmission in the cerebellar cortex. J. Neurosci 32, 11132–11143. [PubMed: 22875944]

Egawa K, Kitagawa K, Inoue K, Takayama M, Takayama C, Saitoh S, Kishino T, Kitagawa M, and Fukuda A (2012). Decreased tonic inhibition in cerebellar granule cells causes motor dysfunction in a mouse model of Angelman syndrome. Sci. Transl. Med 4, 163ra157.

Farrant M, and Nusser Z (2005). Variations on an inhibitory theme: phasic and tonic activation of GABA(A) receptors. Nat. Rev. Neurosci 6, 215–229. [PubMed: 15738957]

Ge Y, Kang Y, Cassidy RM, Moon KM, Lewis R, Wong ROL, Foster LJ, and Craig AM (2018). Clptm1 Limits Forward Trafficking of $GABA_A$ Receptors to Scale Inhibitory Synaptic Strength. Neuron 97, 596–610.e8. [PubMed: 29395912]

Gentet LJ, Stuart GJ, and Clements JD (2000). Direct measurement of specific membrane capacitance in neurons. Biophys. J 79, 314–320. [PubMed: 10866957]

Glykys J, and Mody I (2007). Activation of GABAA receptors: views from outside the synaptic cleft. Neuron 56, 763–770. [PubMed: 18054854]

Glykys J, Mann EO, and Mody I (2008). Which GABA(A) receptor subunits are necessary for tonic inhibition in the hippocampus? J. Neurosci 28, 1421–1426. [PubMed: 18256262]

Han W, Li J, Pelkey KA, Pandey S, Chen X, Wang YX, Wu K, Ge L, Li T, Castellano D, et al. (2019). Shisa7 is a $GABA_A$ receptor auxiliary subunit controlling benzodiazepine actions. Science 366, 246–250. [PubMed: 31601770]

Han W, Shepard RD, and Lu W (2021). Regulation of $GABA_A$Rs by Transmembrane Accessory Proteins. Trends Neurosci. 44, 152–165. [PubMed: 33234346]

Hartman KN, Pal SK, Burrone J, and Murthy VN (2006). Activity-dependent regulation of inhibitory synaptic transmission in hippocampal neurons. Nat. Neurosci 9, 642–649. [PubMed: 16582905]

Hausrat TJ, Muhia M, Gerrow K, Thomas P, Hirdes W, Tsukita S, Heisler FF, Herich L, Dubroqua S, Breiden P, et al. (2015). Radixin regulates synaptic GABAA receptor density and is essential for reversal learning and short-term memory. Nat. Commun 6, 6872. [PubMed: 25891999]

Hengen KB, Torrado Pacheco A, McGregor JN, Van Hooser SD, and Turrigiano GG (2016). Neuronal Firing Rate Homeostasis Is Inhibited by Sleep and Promoted by Wake. Cell 165, 180–191. [PubMed: 26997481]

Hernandez CC, XiangWei W, Hu N, Shen D, Shen W, Lagrange AH, Zhang Y, Dai L, Ding C, Sun Z, et al. (2019). Altered inhibitory synapses in de novo GABRA5 and GABRA1 mutations associated with early onset epileptic encephalopathies. Brain 142, 1938–1954. [PubMed: 31056671]

Hildick KL, González-González IM, Jaskolski F, and Henley JM (2012). Lateral diffusion and exocytosis of membrane proteins in cultured neurons assessed using fluorescence recovery and fluorescence-loss photobleaching. J. Vis. Exp (60), 3747. [PubMed: 22395448]

Hines RM, Davies PA, Moss SJ, and Maguire J (2012). Functional regulation of GABAA receptors in nervous system pathologies. Curr. Opin. Neurobiol 22, 552–558. [PubMed: 22036769]

Hodges LM, Fyer AJ, Weissman MM, Logue MW, Haghighi F, Evgrafov O, Rotondo A, Knowles JA, and Hamilton SP (2014). Evidence for linkage and association of GABRB3 and GABRA5 to panic disorder. Neuropsychopharmacology 39, 2423–2431. [PubMed: 24755890]

Holter NI, Zylla MM, Zuber N, Bruehl C, and Draguhn A (2010). Tonic GABAergic control of mouse dentate granule cells during postnatal development. Eur. J. Neurosci 32, 1300–1309. [PubMed: 20846322]

Holth JK, Fritschi SK, Wang C, Pedersen NP, Cirrito JR, Mahan TE, Finn MB, Manis M, Geerling JC, Fuller PM, et al. (2019). The sleep-wake cycle regulates brain interstitial fluid tau in mice and CSF tau in humans. Science 363, 880–884. [PubMed: 30679382]

Hou T, Wang C, Joshi S, O'Hara BF, Gong MC, and Guo Z (2019). Active Time-Restricted Feeding Improved Sleep-Wake Cycle in *db/db* Mice. Front. Neurosci 13, 969. [PubMed: 31619950]

Jacob TC (2019). Neurobiology and Therapeutic Potential of α5-GABA Type A Receptors. Front. Mol. Neurosci 12, 179. [PubMed: 31396049]

Jacob TC, Moss SJ, and Jurd R (2008). GABA(A) receptor trafficking and its role in the dynamic modulation of neuronal inhibition. Nat. Rev. Neurosci 9, 331–343. [PubMed: 18382465]

Janssen MJ, Ade KK, Fu Z, and Vicini S (2009). Dopamine modulation of GABA tonic conductance in striatal output neurons. J. Neurosci 29, 5116–5126. [PubMed: 19386907]

Kilman V, van Rossum MC, and Turrigiano GG (2002). Activity deprivation reduces miniature IPSC amplitude by decreasing the number of postsynaptic GABA(A) receptors clustered at neocortical synapses. J. Neurosci 22, 1328–1337. [PubMed: 11850460]

Lee V, and Maguire J (2014). The impact of tonic GABAA receptor-mediated inhibition on neuronal excitability varies across brain region and cell type. Front. Neural Circuits 8, 3. [PubMed: 24550784]

Li J, Wilkinson B, Clementel VA, Hou J, O'Dell TJ, and Coba MP (2016). Long-term potentiation modulates synaptic phosphorylation networks and reshapes the structure of the postsynaptic interactome. Sci. Signal 9, rs8. [PubMed: 27507650]

Li J, Han W, Pelkey KA, Duan J, Mao X, Wang YX, Craig MT, Dong L, Petralia RS, McBain CJ, and Lu W (2017). Molecular Dissection of Neuroligin 2 and Slitrk3 Reveals an Essential Framework for GABAergic Synapse Development. Neuron 96, 808–826.e8. [PubMed: 29107521]

Liu ZW, Faraguna U, Cirelli C, Tononi G, and Gao XB (2010). Direct evidence for wake-related increases and sleep-related decreases in synaptic strength in rodent cortex. J. Neurosci 30, 8671–8675. [PubMed: 20573912]

Loebrich S, Bähring R, Katsuno T, Tsukita S, and Kneussel M (2006). Activated radixin is essential for GABAA receptor alpha5 subunit anchoring at the actin cytoskeleton. EMBO J. 25, 987–999. [PubMed: 16467845]

Lu W, and Roche KW (2012). Posttranslational regulation of AMPA receptor trafficking and function. Curr. Opin. Neurobiol 22, 470–479. [PubMed: 22000952]

Luscher B, Fuchs T, and Kilpatrick CL (2011). GABAA receptor trafficking-mediated plasticity of inhibitory synapses. Neuron 70, 385–409. [PubMed: 21555068]

Maguire J, and Mody I (2008). GABA(A)R plasticity during pregnancy: relevance to postpartum depression. Neuron 59, 207–213. [PubMed: 18667149]

Maguire JL, Stell BM, Rafizadeh M, and Mody I (2005). Ovarian cycle-linked changes in GABA(A) receptors mediating tonic inhibition alter seizure susceptibility and anxiety. Nat. Neurosci 8, 797–804. [PubMed: 15895085]

Mang GM, Nicod J, Emmenegger Y, Donohue KD, O'Hara BF, and Franken P (2014). Evaluation of a piezoelectric system as an alternative to electroencephalogram/ electromyogram recordings in mouse sleep studies. Sleep (Basel) 37, 1383–1392.

Martin LJ, Bonin RP, and Orser BA (2009). The physiological properties and therapeutic potential of alpha5-GABAA receptors. Biochem. Soc. Trans 37, 1334–1337. [PubMed: 19909271]

Martin LJ, Zurek AA, MacDonald JF, Roder JC, Jackson MF, and Orser BA (2010). Alpha5GABAA receptor activity sets the threshold for long-term potentiation and constrains hippocampus-dependent memory. J. Neurosci 30, 5269–5282. [PubMed: 20392949]

Mohamad FH, and Has ATC (2019). The α5-Containing $GABA_A$ Receptors-a Brief Summary. J. Mol. Neurosci 67, 343–351. [PubMed: 30607899]

Nakahata Y, Eto K, Murakoshi H, Watanabe M, Kuriu T, Hirata H, Moorhouse AJ, Ishibashi H, and Nabekura J (2017). Activation-Dependent Rapid Postsynaptic Clustering of Glycine Receptors in Mature Spinal Cord Neurons. eNeuro 4, 4.

Nakamura Y, Darnieder LM, Deeb TZ, and Moss SJ (2015). Regulation of GABAARs by phosphorylation. Adv. Pharmacol 72, 97–146. [PubMed: 25600368]

Olsen RW, and Sieghart W (2008). International Union of Pharmacology. LXX. Subtypes of gamma-aminobutyric acid(A) receptors: classification on the basis of subunit composition, pharmacology, and function. Update. Pharmacol. Rev 60, 243–260. [PubMed: 18790874]

Pandit S, Lee GS, and Park JB (2017). Developmental changes in $GABA_A$ tonic inhibition are compromised by multiple mechanisms in preadolescent dentate gyrus granule cells. Korean J. Physiol. Pharmacol 21, 695–702. [PubMed: 29200913]

Peng Z, Huang CS, Stell BM, Mody I, and Houser CR (2004). Altered expression of the delta subunit of the GABAA receptor in a mouse model of temporal lobe epilepsy. J. Neurosci 24, 8629–8639. [PubMed: 15456836]

Quirk K, Blurton P, Fletcher S, Leeson P, Tang F, Mellilo D, Ragan CI, and McKernan RM (1996). [3H]L-655,708, a novel ligand selective for the benzodiazepine site of GABAA receptors which contain the alpha 5 subunit. Neuropharmacology 35, 1331–1335. [PubMed: 9014149]

Saliba RS, Kretschmannova K, and Moss SJ (2012). Activity-dependent phosphorylation of GABAA receptors regulates receptor insertion and tonic current. EMBO J. 31, 2937–2951. [PubMed: 22531784]

Serra M, Mostallino MC, Talani G, Pisu MG, Carta M, Mura ML, Floris I, Maciocco E, Sanna E, and Biggio G (2006). Social isolation-induced increase in alpha and delta subunit gene expression is associated with a greater efficacy of ethanol on steroidogenesis and GABA receptor function. J. Neurochem 98, 122–133. [PubMed: 16805802]

Shen H, Gong QH, Aoki C, Yuan M, Ruderman Y, Dattilo M, Williams K, and Smith SS (2007). Reversal of neurosteroid effects at alpha4beta2-delta GABAA receptors triggers anxiety at puberty. Nat. Neurosci 10, 469–477. [PubMed: 17351635]

Shen H, Sabaliauskas N, Sherpa A, Fenton AA, Stelzer A, Aoki C, and Smith SS (2010). A critical role for alpha4betadelta GABAA receptors in shaping learning deficits at puberty in mice. Science 327, 1515–1518. [PubMed: 20299596]

Tononi G, and Cirelli C (2014). Sleep and the price of plasticity: from synaptic and cellular homeostasis to memory consolidation and integration. Neuron 81, 12–34. [PubMed: 24411729]

Turrigiano G (2012). Homeostatic synaptic plasticity: local and global mechanisms for stabilizing neuronal function. Cold Spring Harb. Perspect. Biol 4, a005736. [PubMed: 22086977]

Turrigiano GG, and Nelson SB (2004). Homeostatic plasticity in the developing nervous system. Nat. Rev. Neurosci 5, 97–107. [PubMed: 14735113]

Turrigiano GG, Leslie KR, Desai NS, Rutherford LC, and Nelson SB (1998). Activity-dependent scaling of quantal amplitude in neocortical neurons. Nature 391, 892–896. [PubMed: 9495341]

Vithlani M, Terunuma M, and Moss SJ (2011). The dynamic modulation of GABA(A) receptor trafficking and its role in regulating the plasticity of inhibitory synapses. Physiol. Rev 91, 1009–1022. [PubMed: 21742794]

Wang DS, Zurek AA, Lecker I, Yu J, Abramian AM, Avramescu S, Davies PA, Moss SJ, Lu WY, and Orser BA (2012). Memory deficits induced by inflammation are regulated by α5-subunit-containing GABAA receptors. Cell Rep. 2, 488–496. [PubMed: 22999935]

Wang Z, Ma J, Miyoshi C, Li Y, Sato M, Ogawa Y, Lou T, Ma C, Gao X, Lee C, et al. (2018). Quantitative phosphoproteomic analysis of the molecular substrates of sleep need. Nature 558, 435–439. [PubMed: 29899451]

Woo J, Min JO, Kang DS, Kim YS, Jung GH, Park HJ, Kim S, An H, Kwon J, Kim J, et al. (2018). Control of motor coordination by astrocytic tonic GABA release through modulation of excitation/inhibition balance in cerebellum. Proc. Natl. Acad. Sci. USA 115, 5004–5009. [PubMed: 29691318]

Wu Z, Guo Z, Gearing M, and Chen G (2014). Tonic inhibition in dentate gyrus impairs long-term potentiation and memory in an Alzheimer's [corrected] disease model. Nat. Commun 5, 4159. [PubMed: 24923909]

Zhang N, Wei W, Mody I, and Houser CR (2007). Altered localization of GABA(A) receptor subunits on dentate granule cell dendrites influences tonic and phasic inhibition in a mouse model of epilepsy. J. Neurosci 27, 7520–7531. [PubMed: 17626213]

Zou G, Chen Q, Chen K, Zuo X, Ge Y, Hou Y, Pan T, Pan H, Liu D, Zhang L, and Xiong W (2019). Human Hyperekplexic Mutations in Glycine Receptors Disinhibit the Brainstem by Hijacking $GABA_A$ Receptors. iScience 19, 634–646. [PubMed: 31450193]

Zurek AA, Yu J, Wang DS, Haffey SC, Bridgwater EM, Penna A, Lecker I, Lei G, Chang T, Salter EW, and Orser BA (2014). Sustained increase in α5GABAA receptor function impairs memory after anesthesia. J. Clin. Invest 124, 5437–5441. [PubMed: 25365226]

Highlights

- Shisa7 is critical for the regulation of tonic inhibition in hippocampal neurons
- PKA phosphorylates Shisa7 to modulate α5-$GABA_AR$ exocytosis and tonic inhibition
- Shisa7 is important for activity-dependent regulation of tonic inhibition
- The sleep/wake cycle regulates tonic inhibition in a Shisa7-dependent manner

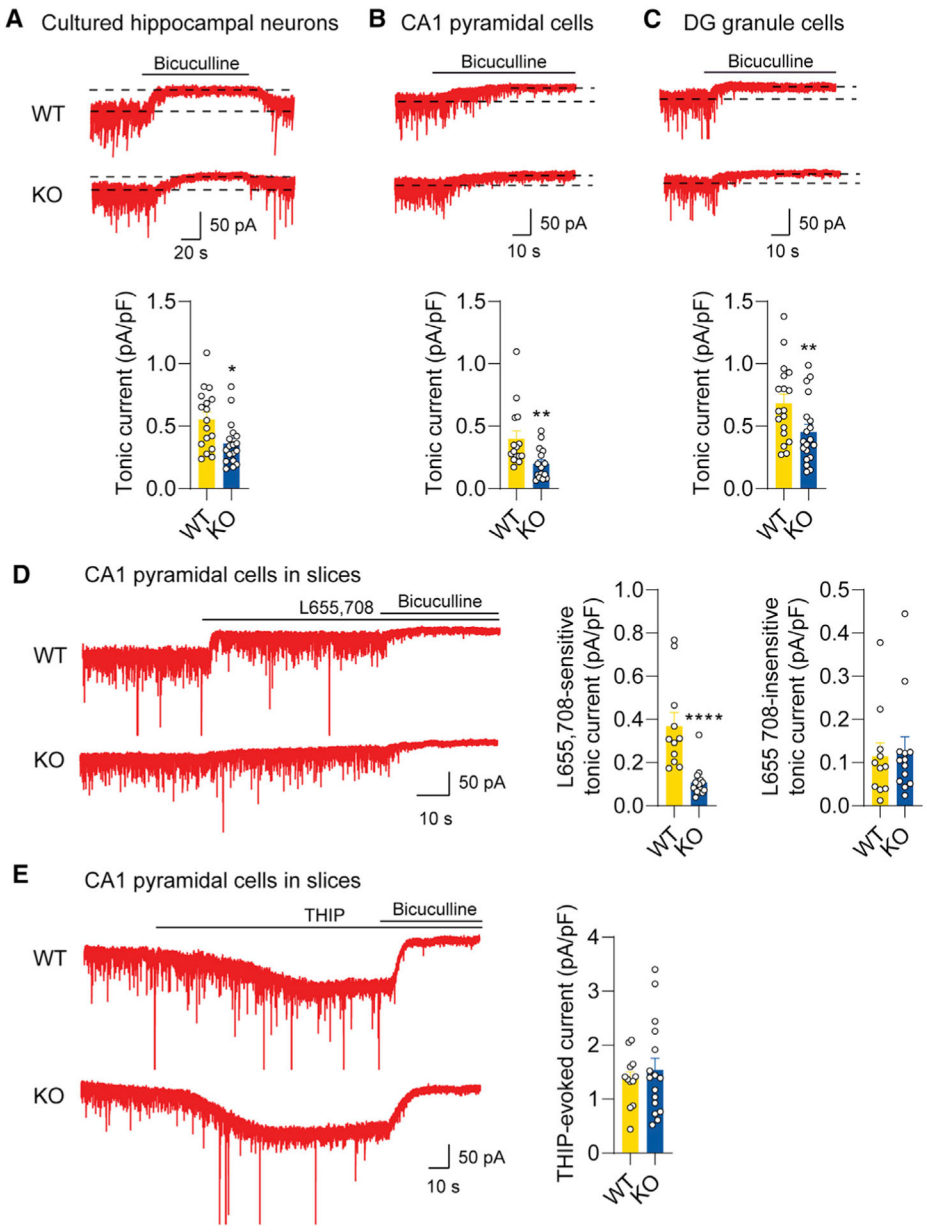

Figure 1. Tonic inhibitory currents are reduced in Shisa7 KO hippocampal neurons

(A) Representative traces showing tonic currents in cultured hippocampal neurons prepared from WT (top) and Shisa7 KO (bottom) animals. Tonic currents were revealed by the shift in holding currents after blocking $GABA_A$Rs with bicuculline (BIC; 20 μM). Bar graphs showing tonic currents in Shisa7 KO neurons were significantly reduced as compared to those in WT neurons (WT, n = 17; KO, n = 18, Mann-Whitney *U* test, p = 0.011).

(B and C) Representative traces and bar graphs showing tonic currents were reduced in CA1 pyramidal neurons (B) and in dentate gyrus (DG) granule cells (C) in acute hippocampal slices prepared from Shisa7 KO mice as compared to WT mice (n = 15–19 for each group; CA1 pyramidal neurons: Mann-Whitney *U* test, p = 0.0049; DG granule cells: t test, p = 0.0012).

(D) Shisa7 KO reduced α5-$GABA_A$Rs-mediated tonic inhibition in CA1 pyramidal neurons in acute hippocampal slices. L655,708 (100 nM), an inverse agonist of α5-$GABA_A$Rs, was applied to block α5-mediated tonic currents before blocking all $GABA_A$Rs with BIC during recording. L-655,708-sensitive components, but not L-655,708-insensitive components, of tonic currents were significantly reduced in Shisa7 KO CA1 neurons (WT, n = 11; KO, n = 14, Mann-Whitney *U* test, $p < 0.0001$).

(E) Shisa7 KO had no effect on δ-$GABA_A$R-mediated tonic inhibition in hippocampal CA1 neurons. THIP (10 μM), a $GABA_A$R agonist with a preference for δ-containing receptors, evoked similar amount of currents in WT and Shisa7 KO CA1 neurons (WT, n = 12; KO, n = 15).

*$p < 0.05$, **$p < 0.01$, and ****$p < 0.0001$. All data are presented as mean ± SEM. See also Figure S1.

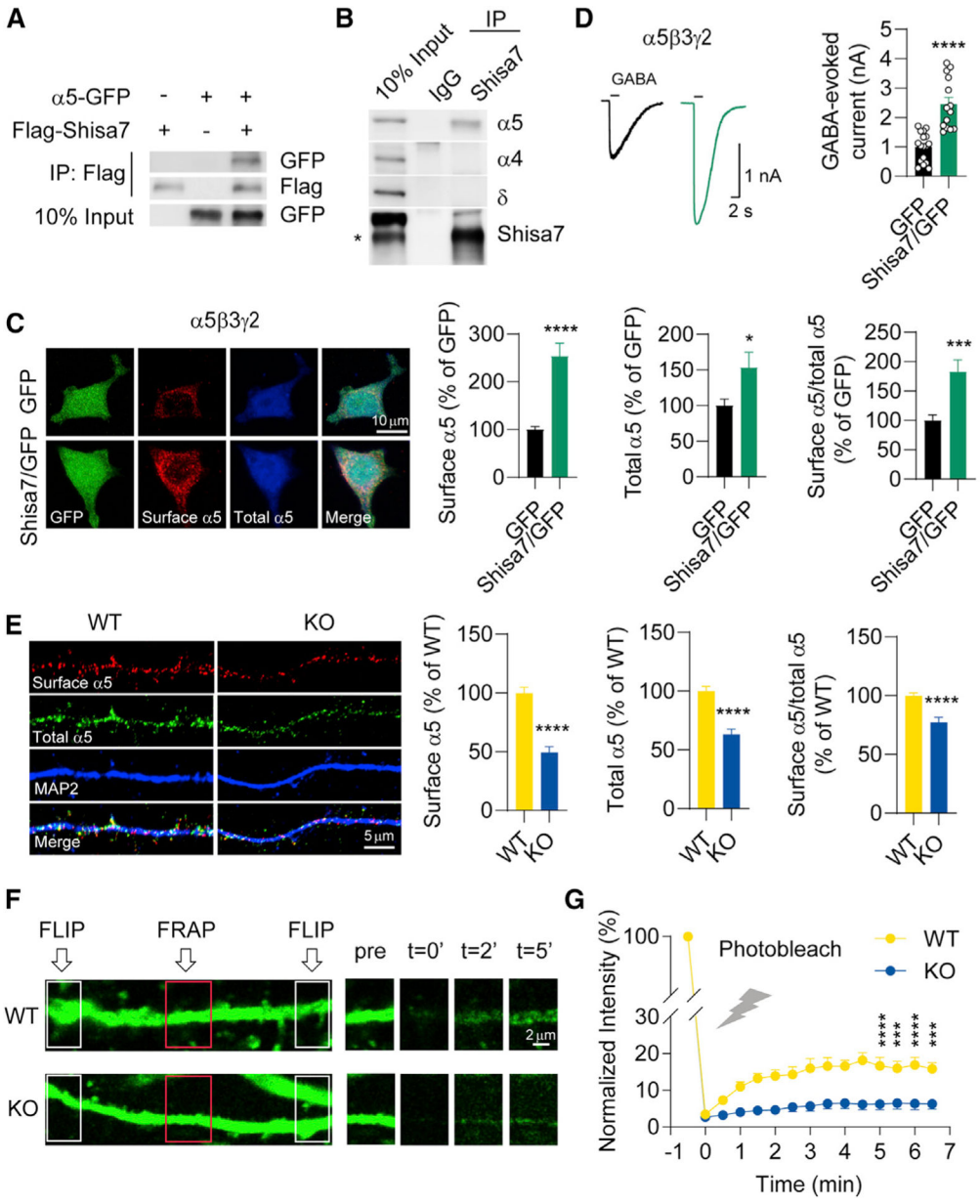

Figure 2. Shisa7 interacts with α5-GABA$_A$Rs and regulates receptor trafficking

(A) Shisa7 interacted with α5 in HEK293T cells. HEK293T cells were transfected with Flag-Shisa7, α5-GFP, or both Flag-Shisa7 and α5-GFP. Cell lysates were subjected to immunoprecipitation and immunoblotting assays (n = 3 independent experiments).

(B) α5, but not α4 or δ, subunit was co-immunoprecipitated with Shisa7 in detergent-solubilized mouse hippocampal lysates. Asterisk indicates the Shisa7 band (n = 3 independent experiments).

(C) Co-expression of α5β3γ2 with Shisa7-IRES-GFP (Shisa7/GFP), but not GFP, increased surface levels, total levels, and surface to total ratio of α5 expression (GFP, n = 23; Shisa7/GFP, n = 27; surface α5: t test, $p < 0.0001$; total α5: Mann-Whitney *U* test, $p = 0.0298$; surface α5/ total α5: t test, $p = 0.0009$).

(D) GABA-evoked α5β3γ2-mediated whole-cell currents were significantly increased in HEK293T cells co-expressing Shisa7/GFP. (GFP, n = 17; Shisa7/GFP, n = 14, t test, p = 0.0001).

(E) Immunostaining (left) and summary graphs (right) showing surface and total α5 expression were reduced in Shisa7 KO neurons (WT, n = 22; KO, n = 20; surface α5: Mann-Whitney *U* test, p < 0.0001; total α5: Mann-Whitney *U* test, p < 0.0001; surface α5/total α5: Mann-Whitney *U* test, p < 0.0001).

(F) Representative images (left) of SEP-α5 fluorescence and the regions of the neuronal dendrites used for the fluorescence recovery after photobleaching (FRAP) and fluorescence loss in photobleaching (FLIP) experiments. Repetitive photobleaching (FLIP, white box) occurred at regions bilateral to the central FRAP region (red box). Each column (right) represents before (pre), immediately after (t = 0′), and at 2 min (t = 2′) and 5 min (t = 5′) after photobleaching in each condition.

(G) Normalized fluorescence recovery curves showing significantly less newly inserted α5 on the cell surface in Shisa7 KO neurons than in WT neurons 5 min after photobleaching, indicating that α5-$GABA_A$Rs exocytosis was impaired inShisa7 KO neurons (WT, n = 6; KO, n = 8, two-way ANOVA with Tukey's multiple comparison test. t = 5′: p < 0.0001; t = 5.5′: p = 0.0002; t = 6′: p < 0.0001; t = 6.5′: p = 0.0002).

*p < 0.05, ***p < 0.001, and ****p < 0.0001. All data are presented as mean ± SEM. See also Figure S2.

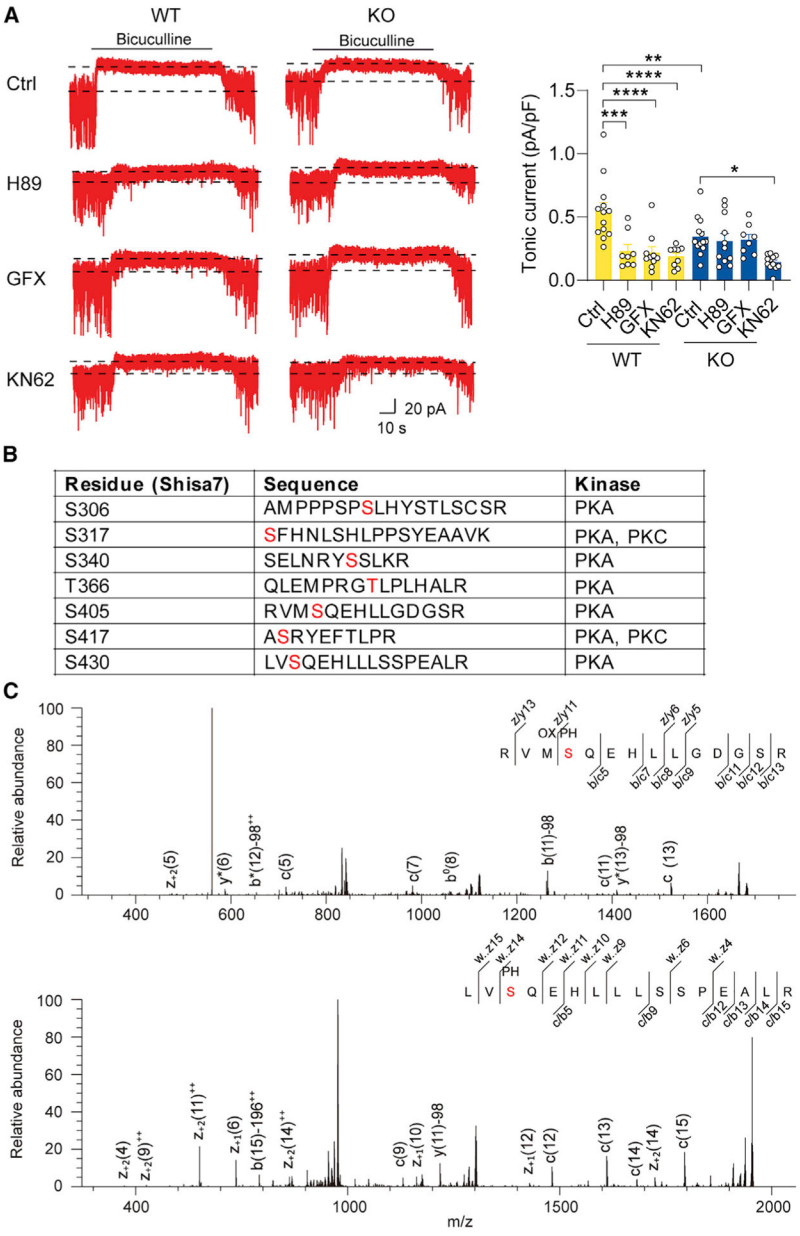

Residue (Shisa7)	Sequence	Kinase
S306	AMPPPSPSLHYSTLSCSR	PKA
S317	SFHNLSHLPPSYEAAVK	PKA, PKC
S340	SELNRYSSLKR	PKA
T366	QLEMPRGTLPLHALR	PKA
S405	RVMSQEHLLGDGSR	PKA
S417	ASRYEFTLPR	PKA, PKC
S430	LVSQEHLLLSSPEALR	PKA

Figure 3. Protein kinases regulate tonic inhibition

(A) PKA or PKC regulated tonic inhibition through Shisa7. PKA inhibitor H89 (20 μM), PKC inhibitor GF109203X (GFX, 200 nM), or CaMKII inhibitor KN62 (3 μM) reduced tonic currents in WT neurons compared to control (Ctrl); however, the effects of H89 and GFX, but not KN62, on tonic currents were abolished in Shisa7 KO neurons (n = 8–13 for each group, two-way ANOVA, $F_{3, 76} = 4.435$, $p = 0.0063$ with Tukey's multiple comparison test; WT: Ctrl versus KO: Ctrl, $p = 0.0061$; WT: Ctrl versus WT: H89, $p = 0.0002$; WT: Ctrl versus WT: H89, $p < 0.0001$; WT: Ctrl versus WT: KN62, $p < 0.0001$; KO: Ctrl versus KO: KN62, $p = 0.0105$).

(B) MS analysis for phosphorylation of Shisa7 C-tail by PKA and PKC. The phosphorylated residues in identified peptide sequences were highlighted in red (n = 3 independent experiments).

(C) MS/MS spectrum of phosphorylated Shisa7 peptides 401-RVMSQEHLLGDGSR-416 (top) and 427-LVSQEHLLSSPEALR-443 (bottom) found in mouse hippocampal lysates. Phosphorylated residues (S405 and S430) are highlighted in red (n = 3 independent experiments).

*$p < 0.05$, ***$p < 0.001$, and ****$p < 0.0001$. All data are presented as mean ± SEM.

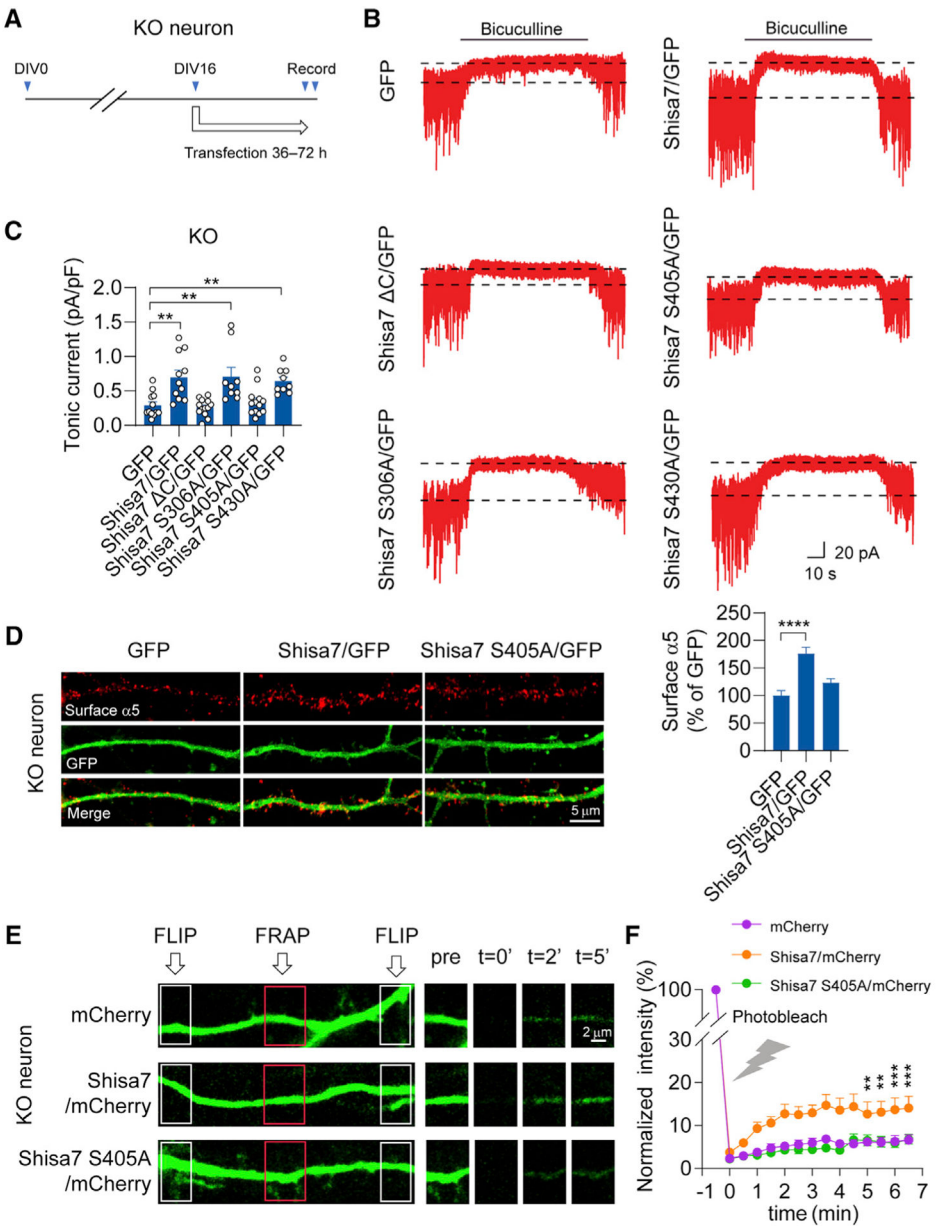

Figure 4. PKA phosphorylates Shisa7 to regulate α5 exocytosis and tonic inhibition

(A) Experimental design. Neurons were transfected at 16 days *in vitro* (DIV16) for 36–72 h and then recorded for tonic currents.

(B and C) Representative traces (B) and summary graphs (C) showing Shisa7, Shisa7 S306A, or Shisa7 S430A, but not Shisa7 mutants lacking the C-tail (Shisa7 ΔC) or Shisa7 S405A, restored tonic current deficits in Shisa7 KO neurons (n = 9–13 for each group, Kruskal-Wallis test with Dunnett's multiple comparisons test; GFP versus Shisa7/GFP, p = 0.0052; GFP versus Shisa7 S306A /GFP, p = 0.0075; GFP versus Shisa7 S430/GFP, p = 0.0027).

(D) Immunostaining (left) and summary graphs (right) showing Shisa7, but not Shisa7 S405A, restored decreased surface α5 expression in Shisa7 KO neurons (n = 16–24 for each

group, Kruskal-Wallis test with Dunnett's multiple comparisons test. GFP versus Shisa7/GFP, $p < 0.0001$).

(E) Representative images (left) of SEP-α5 fluorescence and the regions of the neuronal dendrites used for the FRAP-FLIP experiments. Repetitive photobleaching (FLIP, white box) occurred at regions bilateral to the central FRAP region (red box). Each column (right) represents before (pre), immediately after ($t = 0'$), and at 2 min ($t = 2'$) and 5 min ($t = 5'$) after photobleaching in each condition.

(F) Normalized fluorescence recovery curves showing Shisa7, but not Shisa7 S405A, rescued α5 exocytosis deficits in Shisa7 KO neurons ($n = 6–8$ for each group, two-way ANOVA, $F_{28, 238} = 3.598$, $p < 0.0001$ with Dunnett's multiple comparison test; $t = 5'$: mCherry versus Shisa7/mCherry, $p = 0.0029$; $t = 5.5'$: mCherry versus Shisa7/mCherry, $p = 0.0013$; $t = 6'$: mCherry versus Shisa7/mCherry, $p = 0.0006$; $t = 6.5'$: mCherry versus Shisa7/mCherry, $p = 0.0005$).

**$p < 0.01$, ***$p < 0.001$, and ****$p < 0.0001$. All data are presented as mean ± SEM. See also Figure S3.

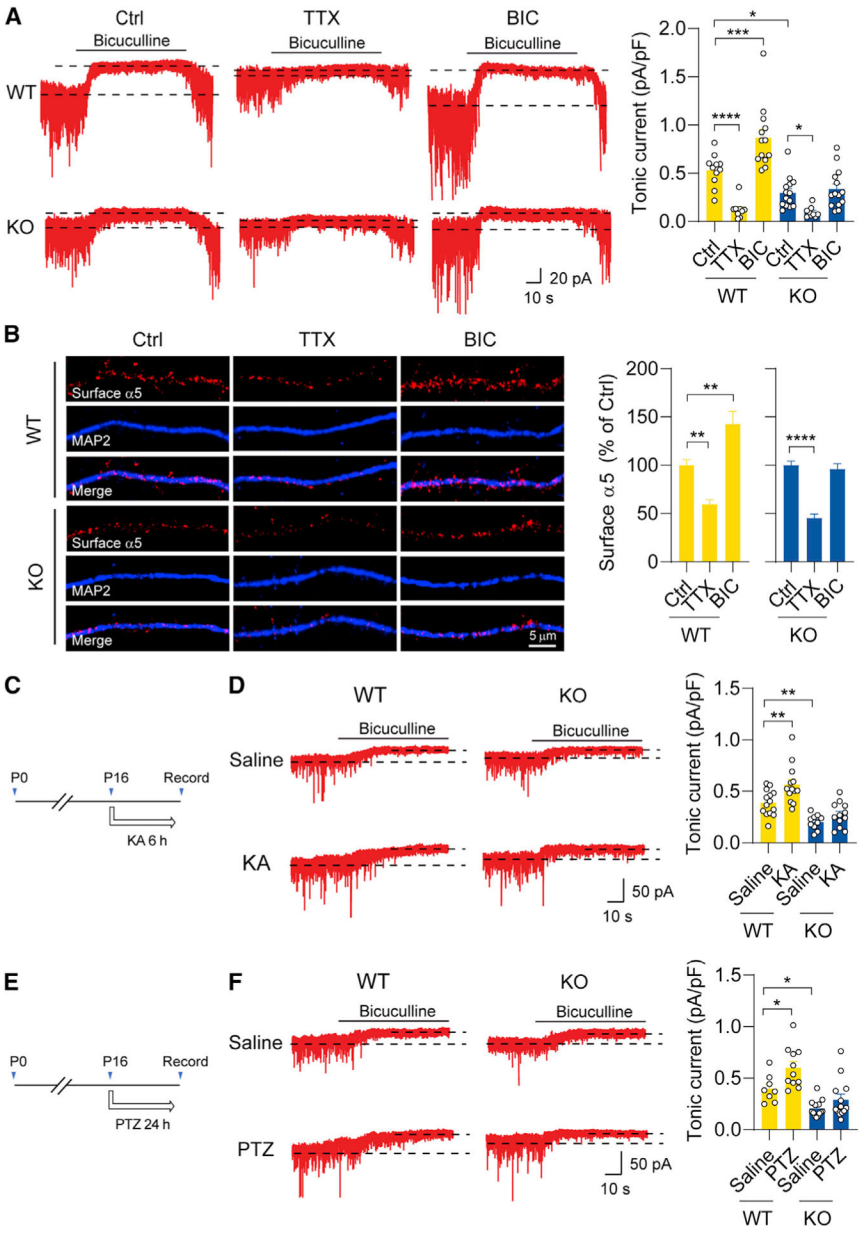

Figure 5. Shisa7 is required for homeostatic potentiation of tonic inhibition *in vitro* and *in vivo*

(A) Tonic currents in WT hippocampal neurons were significantly increased following BIC (40 μM) treatment and decreased following TTX (1 μM) treatment. Shisa7 KO blocked BIC-induced potentiation of tonic currents (n = 9–14 for each group, two-way ANOVA, $F_{2, 66}$ = 9.742, p = 0.0002 with Sidak's multiple comparison test; WT: Ctrl versus KO: Ctrl, p = 0.0111; WT: Ctrl versus WT: TTX, p < 0.0001; WT: Ctrl versus WT: BIC, p = 0.0003; KO: Ctrl versus KO: TTX, p = 0.0342).

(B) Surface α5 was significantly increased following BIC treatment and decreased following TTX treatment in WT hippocampal neurons. Shisa7 KO blocked BIC-induced increase of surface α5 (n = 17–26 for each group, WT: one-way ANOVA, F = 23.46, p < 0.0001 with Dunnett's multiple comparisons test; WT: Ctrl versus WT: TTX, p = 0.0049; WT: Ctrl

versus WT: BIC, p = 0.0037; KO: one-way ANOVA, F = 37.49, p < 0.0001 with Dunnett's multiple comparisons test; KO: Ctrl versus KO: TTX, p < 0.0001).

(C and E) Experimental design. Mice were injected with kainic acid (KA; 4 mg/kg) or pentylenetetrazol (PTZ; 40 mg/kg) at P16. CA1 cells were recorded 6 h after KA injection or 24 h after PTZ injection.

(D) Shisa7 KO blocked KA-induced potentiation of tonic currents in CA1 neurons (n = 10–14 for each group, two-way ANOVA, $F_{1, 45} = 9.747$, p = 0.0031 with Sidak's multiple comparison test; WT: saline versus KO: saline, p = 0.0037; WT: saline versus WT: KA, p = 0.0032).

(F) Shisa7 KO blocked PTZ-induced potentiation of tonic currents in CA1 neurons (n = 8–13 for each group, two-way ANOVA, $F_{1, 41} = 9.040$, p = 0.0045 with Sidak's multiple comparison test; WT: saline versus KO: saline, p = 0.0175; WT: saline versus WT: PTZ, p = 0.0189).

*p < 0.05, **p < 0.01, ***p < 0.001, and ****p < 0.0001. All data are presented as mean ± SEM. See also Figure S4.

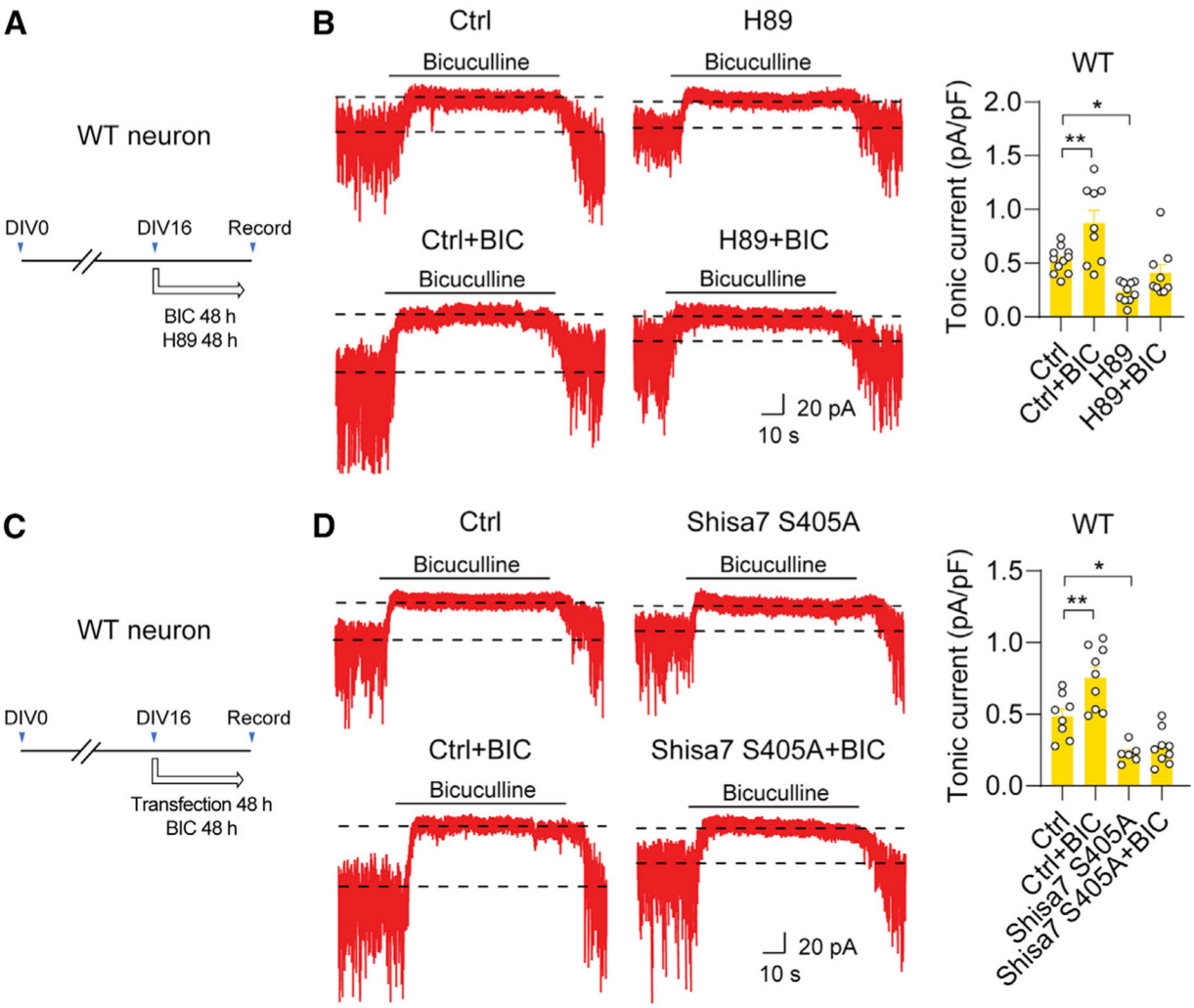

Figure 6. Shisa7 S405 is required for homeostatic potentiation of tonic inhibition

(A) Experimental design. WT hippocampal neurons were treated with BIC (40 μM), H89 (1 μM), or both for 48 h and then recorded for tonic currents.

(B) H89 abolished BIC-induced potentiation of tonic currents in WT hippocampal neurons (n = 9–11 for each group, one-way ANOVA, $F = 13.72$, $p < 0.0001$ with Tukey's multiple comparisons test; Ctrl versus Ctrl + BIC, $p = 0.0084$; Ctrl versus H89, $p = 0.0213$).

(C) Experimental design. WT hippocampal neurons were transfected with Shisa7 S405A at DIV16 and then treated with BIC (40 μM) for 48 h before recording.

(D) Expression of Shisa7 S405A blocked BIC-induced potentiation of tonic currents in WT hippocampal neurons (n = 6–9 for each group, one-way ANOVA, $F = 20.30$, $p < 0.0001$ with Tukey's multiple comparisons test; Ctrl versus Ctrl + BIC, $p = 0.0061$; Ctrl versus Shisa7 S306A, $p = 0.0212$).

*$p < 0.05$ and **$p < 0.01$. All data are presented as mean ± SEM.

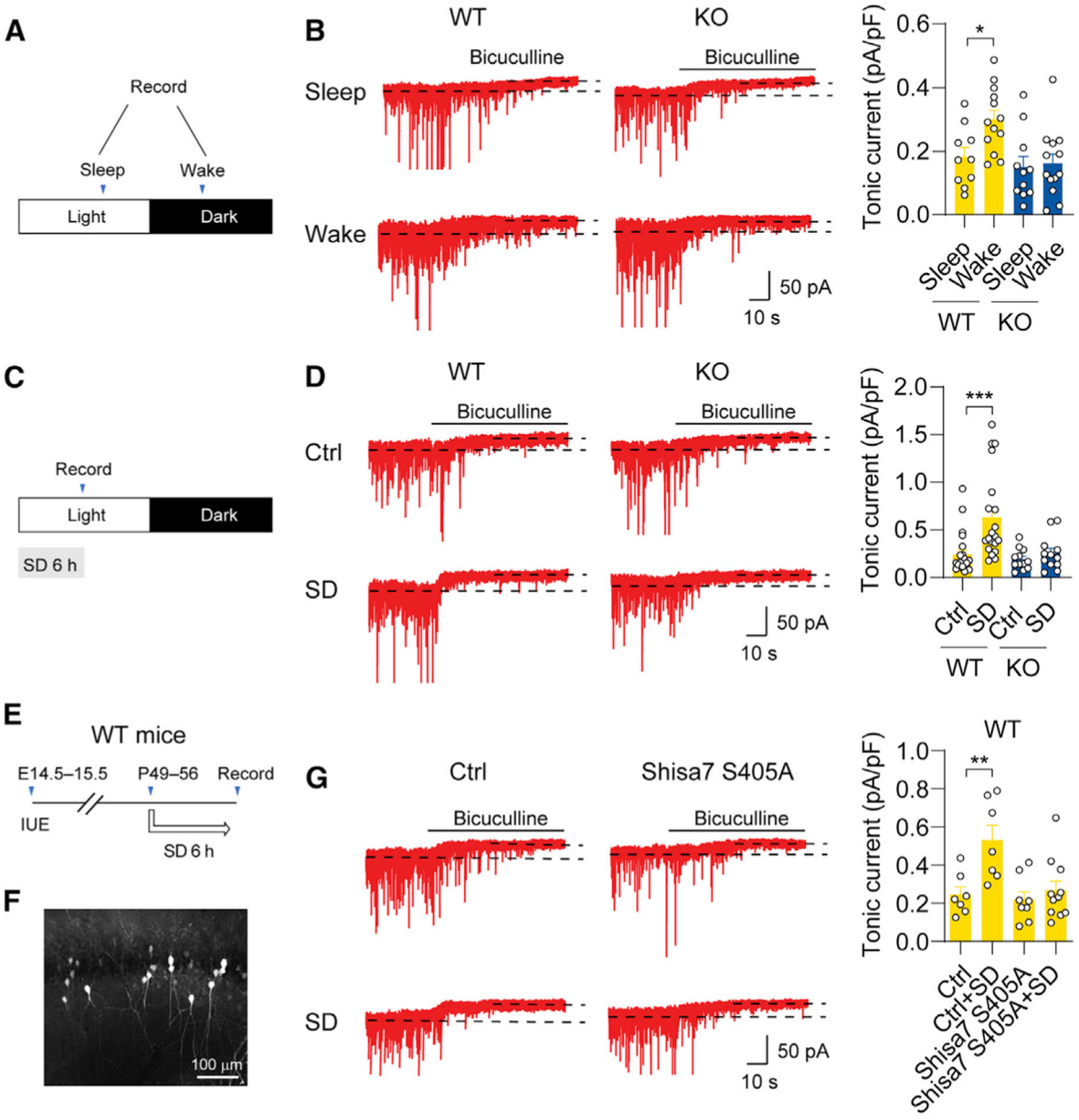

Figure 7. Tonic inhibition changes over the daily sleep/wake cycle in a Shisa7-dependent manner

(A) Experimental design. Sleep/wake patterns in young adult mice (P42–P56) were recorded based on the following criteria: “sleep mice” were asleep for at least 65% of the previous 4 h (≥60% per hour), whereas “wake mice” were awake for at least 75% of the previous 4 h (≥70% per hour).

(B) Tonic inhibition was increased in CA1 neurons in WT mice in wake, and Shisa7 KO abolished the increase of tonic inhibition associated with the wake phase. (n = 10–13 for each group, two-way ANOVA, $F_{1, 43} = 4.405$, $p = 0.0417$ with Sidak’s multiple comparison test, WT: Sleep versus WT: Wake, $p = 0.02$)

(C) Experimental design. Mice (P42–56) were sleep-deprived at the beginning of the light phase for 6 h before recording.

(D) Sleep deprivation (SD) increased tonic inhibition in CA1 neurons in WT mice, and Shisa7 KO abolished SD-induced enhancement of tonic currents (n = 12–22 for each group, two-way ANOVA, $F_{1, 62} = 9.003$, p = 0.0039 with Sidak's multiple comparison test, WT: Ctrl versus WT: SD, p = 0.0001)

(E) Experimental design. *In utero* electroporation (IUE) to express Shisa7 S405A was performed at E14.5–15.5. Whole-cell recordings in CA1 neurons were performed at P49–P56 after 6-h SD.

(F) Representative image showing mosaic expression of Shisa7 S405A-IRES-GFP in CA1 neurons in an acute hippocampal slice.

(G) Expression of Shisa7 S405A blocked SD-induced potentiation of tonic currents in WT CA1 neurons (n = 7–11 for each group, one-way ANOVA, F = 6.409, p = 0.0018 with Tukey's multiple comparisons test, Ctrl versus Ctrl + SD, p = 0.0086).

*p < 0.05 and **p < 0.01. All data are presented as mean ± SEM. See also Figures S5–S7.

KEY RESOURCES TABLE

REAGENT or RESOURCE	SOURCE	IDENTIFIER
Antibodies		
Rabbit Polyclonal Anti-Shisa7	GenScript	Han et al., 2019
Mouse Monoclonal Anti-Flag M2, Clone M2	Sigma-Aldrich	Cat# F3165; RRID: AB_259529
Rabbit Polyclonal Anti-GFP	Sigma-Aldrich	Cat# G1544; RRID:AB_439690
Mouse Monoclonal Anti-GABA(A) α5 Receptor	James Trimmer, University of California at Davis	Cat # N415/24; RRID: AB_2750794
Rabbit Polyclonal Anti-GABA(A) δ Receptor	Alomone Labs	Cat # AGA-014; RRID: AB_2340938
Rabbit Polyclonal Anti-GABA(A) α4 Receptor	Alomone Labs	Cat # AGA-008; RRID: AB_10917596
Rabbit Polyclonal Anti-GABA(A) α5 Receptor	Synaptic Systems	Cat# 224503; RRID: AB_2619944
Rabbit IgG	Sigma-Aldrich	Cat# I8140; RRID: AB_1163661
Mouse Monoclonal Anti-Gephyrin	Synaptic Systems	Cat# 147011; RRID: AB_887717
Chicken Polyclonal Anti-MAP2	Aves Labs	Cat# MAP; RRID: AB_2313549
Alexa 647 goat anti-chicken IgG (H+L)	Thermo Fisher Scientific	Cat# A-21449; RRID: AB_2535866
Alexa 488 goat anti-rabbit IgG (H+L)	Jackson ImmunoResearch Labs	Cat# 111-546-003; RRID: AB_2338053
Alexa 488 goat anti-mouse IgG (H+L)	Jackson ImmunoResearch Labs	Cat# 115-546-003; RRID: AB_2338859
Alexa 555 donkey anti-rabbit IgG (H+L)	Thermo Fisher Scientific	Cat# A-31572; RRID: AB_162543
Chemicals, peptides, and recombinant proteins		
NeuroMag reagent	Oz Biosciences	Cat# NM51000
CalPho Mammalian Transfection Kit	Takara	Cat# 631312
Lipofectamine 3000	Thermo Fisher Scientific	Cat# L3000008
Bicuculline	Abcam	Cat# ab120110
L655,708	Sigma-Aldrich	Cat# L9787
4,5,6,7-tetrahydroisoxazolo(5,4-c) pyridin- 3-ol (THIP)	Santa Cruz	Cat# SC204342
H89	Abcam	Cat# ab120341
KN62	Abcam	Cat# ab120421
GF109203X	Abcam	Cat# ab144264
D-APV	Abcam	Cat# ab120003
DNQX	Alomone labs	Cat# D-131
Tetrodotoxin (TTX)	Alomone Labs	Cat#: T-550
Anti-Flag M2 affinity gel	Sigma-Aldrich	Cat# A2220; RRID: AB_10063035
Phosphatase Inhibitor Cocktail	Thermo Fisher Scientific	Cat# 78420
Protease inhibitor cocktail	Roche	Cat# 05892791001
Kainic acid	Abcam	Cat# ab120100
Pentylenetetrazole (PTZ)	Sigma-Aldrich	Cat# P6500
Pierce Glutathione Agarose	Thermo Fisher Scientific	Cat# 16101
Dynabead Protein G	Thermo Fisher Scientific	Cat# 10003D
cAMP-Dependent Protein Kinase, Catalytic Subunit	Promega	Cat# V5161
Protein Kinase C	Promega	Cat# V5261
Experimental models: cell lines		
Primary cultures of hippocampal neurons	This paper	N/A

REAGENT or RESOURCE	SOURCE	IDENTIFIER
HEK293T	ATCC	Cat# CRL-1126
Experimental Models: Organisms/Strains		
C57BL/6N mice	Charles River	Cat# 027
Shisa7 germline knockout mice	Han et al., 2019	N/A
Recombinant DNA		
pCAGGs-Shisa7-IRES-GFP	Han et al., 2019	N/A
pcDNA3-Flag-Shisa7	Han et al., 2019	N/A
α5-GFP	Addgene	Cat# 118956
Superecliptic pHluorin (SEP)-α1	Addgene	Cat# 49168
$GABA_AR$ α5	Dr. Joseph Lynch (University of Queensland, Australia)	N/A
$GABA_AR$ β3	Dr. Joseph Lynch (University of Queensland, Australia)	N/A
$GABA_AR$ γ2L	Dr. Joseph Lynch (University of Queensland, Australia)	N/A
pGEX-4T-Shisa7(211–349)	This paper	N/A
pGEX-4T-Shisa7(347–558)	This paper	N/A
pCAGGs-Shisa7 S306A-IRES-GFP	This paper	N/A
pCAGGs-Shisa7 S405A-IRES-GFP	This paper	N/A
pCAGGs-Shisa7 S430A-IRES-GFP	This paper	N/A
pCAGGs-Shisa7 S405D-IRES-GFP	This paper	N/A
pCAGGs-Shisa7-IRES-mCherry	This paper	N/A
pCAGGs-Shisa7 S405A-IRES-mCherry	This paper	N/A
SEP-α5	This paper	N/A
Software and algorithms		
ImageJ	NIH	https://imagej.nih.gov/ij/
GraphPad Prism 8.0	GraphPad	https://www.graphpad.com
Igor Pro	Wavemetrics	https://www.wavemetrics.com
SleepStats Data Explorer	Signal Solutions	https://www.sigsoln.com/